Autophagy 10:2, 311–330; February 2014; © 2014 Landes Bioscience

Selective inhibition of IFNG-induced autophagy by *Mir155*- and *Mir31*-responsive WNT5A and SHH signaling

Sahana Holla,[1] Mariola Kurowska-Stolarska,[2] Jagadeesh Bayry,[3] and Kithiganahalli Narayanaswamy Balaji[1,*]

[1]Department of Microbiology and Cell Biology; Indian Institute of Science; Bangalore, Karnataka India; [2]Institute of Infection, Immunity and Inflammation; University of Glasgow; Glasgow, Scotland UK; [3]Centre de Recherche des Cordeliers; Institut National de la Santé et de la Recherche Médicale; Paris, France

Keywords: autophagy, IFNG, WNT-SHH signaling, microRNA, lipoxygenase

Abbreviations: AGO2, argonaute RISC catalytic component 2; ALOX, arachidonate lipoxygenase; BMDMs, bone marrow-derived macrophages; ChIP, chromatin immunoprecipitation; DN, dominant negative; IFNG, interferon, gamma; JAK, janus kinase; LX, lipoxins; MAP1LC3, microtubule-associated protein 1 light chain 3; MTOR, mechanistic target of rapamycin; PLD1, phospholipase D1, phosphatidylcholine-specific; PI3K, class I phosphoinositide 3-kinase; PtdIns3K, class III phosphatidylinositol 3-kinase; RPS6KB2, ribosomal protein S6 kinase, 70 kDa, polypeptide 2; SHH, sonic hedgehog; STAT1, signal transducer and activator of transcription 1; TCF, transcription factor family; TLR, toll-like receptor; ULK, unc-51 like autophagy activating kinase

Autophagy is one of the major immune mechanisms engaged to clear intracellular infectious agents. However, several pathogens have evolved strategies to evade autophagy. Here, we demonstrated that *Mycobacteria*, *Shigella,* and *Listeria* but not *Klebsiella*, *Staphylococcus,* and *Escherichia* inhibit IFNG-induced autophagy in macrophages by evoking selective and robust activation of WNT and SHH pathways via MTOR. Utilization of gain- or loss-of-function analyses as well as *mir155*-null macrophages emphasized the role of MTOR-responsive epigenetic modifications in the induction of *Mir155* and *Mir31*. Importantly, cellular levels of PP2A, a phosphatase, were regulated by *Mir155* and *Mir31* to fine-tune autophagy. Diminished expression of PP2A led to inhibition of GSK3B, thus facilitating the prolonged activation of WNT and SHH signaling pathways. Sustained WNT and SHH signaling effectuated the expression of anti-inflammatory lipoxygenases, which in tandem inhibited IFNG-induced JAK-STAT signaling and contributed to evasion of autophagy. Altogether, these results established a role for new host factors and inhibitory mechanisms employed by the pathogens to limit autophagy, which could be targeted for therapeutic interventions.

Introduction

Autophagy is primarily a homeostatic mechanism that enables recycling of the cellular cargo or damaged or excess organelles by sequestering them to characteristic double-membrane autophagosomes, which in turn fuse with lysosomes.[1] Mechanistic target of rapamycin (MTOR) is a critical regulator of autophagy, which inhibits the activation of the ULK (unc-51 like autophagy activating kinase) complex required for initiation of autophagy. Stimulation of the ULK complex leads to a cascade of events including activation of class III phosphatidylinositol 3-kinase (PtdIns3K) complexes, ATG9, MAP1LC3 (microtubule-associated protein 1 light chain 3) conjugation systems to form the functional autophagosome.[2,3] Apart from the cues such as nutrient limitation, stress, and starvation, infection-induced autophagy has recently garnered attention.[4,5]

Autophagy contributes to both innate and adaptive immune responses to infections and plays an essential role in restricting intracellular pathogens and delivering pathogen-derived antigens for major histocompatibility complex class II presentation.[6-9] Thus, autophagy acts as one of the major regulatory mechanisms to curtail the infectious agents. However, intracellular pathogens, especially viruses such as herpes simplex virus, human immunodeficiency virus, influenza; and bacteria like *Mycobacteria*, *Shigella*, *Listeria*, exhibit multiple mechanisms to evade autophagy.[10-13] Escape from autophagy includes not only the ability of the pathogen or pathogen-derived antigens such as Shigella T3SS effector IcsB[14] and the Listeria protein ActA[15] to directly modulate the components of autophagy but also the utilization of this machinery for their survival as in the case of several viruses.[12] Further, genome-wide screening studies have indicated the existence of pathogen-induced host macromolecules that could

*Correspondence to: Kithiganahalli Narayanaswamy Balaji; Email: balaji@mcbl.iisc.ernet.in
Submitted: 03/21/2013; Revised: 11/10/2013; Accepted: 11/15/2013
http://dx.doi.org/10.4161/auto.27225

inhibit autophagy during mycobacterial infections.[16] However, the identities of such host signaling molecules and mechanisms by which pathogens modulate autophagy have not been explored in depth.

Recognition of pathogens by pattern-recognition receptors (PRR) such as toll-like receptor (TLR) and subsequent cytokine responses lead to numerous signaling pathways that could modulate the various molecular regulators of autophagy. Interestingly, signaling via TLR4, as well as TLR7 and TLR8 but not TLR2, an important PRR utilized by pathogens such as *Mycobacteria*, *Shigella*, and *Listeria*, induce autophagy,[17] suggesting that these pathogens might use the TLR2 pathway to escape autophagy. Several reports have shown that TLR2 signaling by *Mycobacteria* leads to activation of a gamut of pathways like NOTCH1,[18] WNT,[19] SHH (sonic hedgehog)[20] contributing to the differential regulation of the innate immune response and cytokine milieu.[21] Of note, a recent study reveals the inhibitory effects of HH signaling on autophagy.[22] Further, the Th1 cytokines TNF[23] and IFNG (interferon, gamma)[24,25] that are implicated in protective responses to mycobacteria, could augment autophagy while the Th2 cytokines IL4 and IL13 could inhibit autophagy by modulating the class I phosphoinositide 3-kinase (PI3K) and MTOR signaling.[26] Based on these observations, we hypothesized that pathogens have the ability to differentially regulate the signaling pathways to regulate autophagy.

Here, we demonstrate that bacterial pathogens such as *Mycobacteria*, *Shigella,* and *Listeria* inhibit IFNG-induced autophagy and stimulate robust activation of MTOR-responsive WNT and SHH signaling. GSK3B, a negative regulator and a nodal link between WNT and SHH pathways was ascertained to be regulated by a protein phosphatase, PP2A. The activity of PP2A was marked by MTOR-dependent expression of microRNAs, *Mir155* and *Mir31* as validated by utilization of macrophages derived from *mir155*-null mice or by conventional siRNA or miRNA mimics or overexpression strategies. Importantly, we found that infection-induced WNT and SHH pathways stimulated the production of ALOXs (arachidonate lipoxygenases) that facilitated the ability of the pathogens to inhibit autophagy. Together, we have identified novel molecular mechanisms and host factors that are crucial to control autophagy and help the bacterial pathogens to evade the host immune responses.

Results

MTOR-dependent WNT-SHH signaling regulates autophagy

To investigate the molecular mechanisms of regulation of autophagy by pathogens, we chose a panel of bacteria. *Klebsiella pneumoniae*, *Staphylococcus aureus,* and *Escherichia coli* were previously reported to induce autophagy, whereas, *Mycobacterium bovis* BCG, *Shigella flexneri,* and *Listeria monocytogenes* are known to inhibit autophagy. First, we assessed the ability of these pathogens to modulate IFNG-mediated autophagy in macrophages. As expected, IFNG-induced high levels of autophagy in macrophages as analyzed by the characteristic MAP1LC3 puncta formation and MAP1LC3-II lipidation (**Fig. 1A–C**). Interestingly, IFNG-induced autophagy was significantly inhibited by *M. bovis* BCG, *S. flexneri,* and *L. monocytogenes* whereas the other 3 bacteria did not modulate the process. For further investigations, *M. bovis* BCG was used as a model pathogen while other bacteria were used only for key experiments.

TLR2 is one of the major innate PRRs that mediates the immune response to mycobacteria. We analyzed the role for TLR2 in inhibition of IFNG-induced autophagy. *M. bovis* BCG failed to inhibit IFNG-induced autophagy both in TLR2 dominant negative (DN)-expressing and *tlr2*-deficient macrophages (**Fig. S1A–S1C**). Further, MTOR, an essential regulator of autophagy was phosphorylated and markedly active in *M. bovis* BCG-, *S. flexneri*- and *L. monocytogenes*-infected macrophages as assayed by phosphorylation status of ribosomal protein S6 kinase, 70 kDa, polypeptide 2 (RPS6KB2/p70S6K) at an MTOR-specific phosphorylation site (Thr389) (**Fig. 1D**). Corroborating these results, MTOR-immunoprecipitates from *M. bovis* BCG-, *S. flexneri*- and *L. monocytogenes*-infected macrophages displayed increased MTOR kinase activity as analyzed by ELISA-based activity assays (data not shown). These results indicate MTOR-dependent regulation of autophagy by these pathogens.

Previous reports suggest that mycobacteria activate the TLR2-dependent RAS pathway.[27,28] Further, phosphatidic acid, a product of PLD1 (phospholipase D1, phosphatidylcholine-specific), is a known inducer of MTOR signaling[29] and a role for RAS-induced, PLD1-mediated MTOR activity is also established.[30] Therefore, we examined the role of RAS-, PLD1- and PI3K-mediated MTOR activation during mycobacterial infection. We saw that, pharmacological inhibition of RAS-PLD1-PI3K significantly abrogated *M. bovis* BCG-induced activation of MTOR as assayed by phosphorylation status of RPS6KB2 (Thr389) (**Fig. S1D**). Interestingly, *M. bovis* BCG failed to induce MTOR activation in *tlr2*-deficient macrophages (**Fig. S1D**). *S. flexneri* and *L. monocytogenes* also exhibited

Figure 1 (See opposite page). Bacteria that inhibit autophagy induce MTOR-dependent WNT-SHH signaling. (**A and B**) Murine RAW 264.7 macrophages were transiently transfected with pEGFP-MAP1LC3 and infected with indicated bacteria for 12 h prior to IFNG (200 U/ml) treatment for 2 h. Representative immunofluorescence images are shown (**A**) and the number of cells expressing MAP1LC3 puncta was quantified (**B**). (**C**) Immunoblotting was performed to analyze MAP1LC3-I/-II using lysates obtained from peritoneal macrophages (from C3H/HeJ mice) infected with the indicated bacteria for 12 h prior to IFNG treatment. (**D and E**) show the activation analysis of MTOR-RPS6KB2 (**D**) and expression analysis of WNT-SHH signaling markers (**E**) upon infection of peritoneal macrophages (from C3H/HeJ mice) with the indicated microbes. (**F and G**) Murine RAW 264.7 macrophages were transiently transfected with NT or *Mtor* siRNA or MTOR overexpression or dominant negative constructs and infected with *M. bovis* BCG for 6 h. Transcript (**F**) and protein (**G**) levels of various WNT-SHH signaling markers were determined using quantitative real-time RT-PCR and immunoblotting respectively. All data represent the mean ± SEM for 5 to 6 values from 3 independent experiments, ns = not significant, *$P < 0.05$, **$P < 0.005$, ***$P < 0.0001$ (one-way ANOVA) and all blots are representative of 3 independent experiments. The cells were infected with bacteria at MOI 1:10 in the experiments. Med, medium; NT, nontargeting; DN, dominant negative. Scale bar: 5 μm.

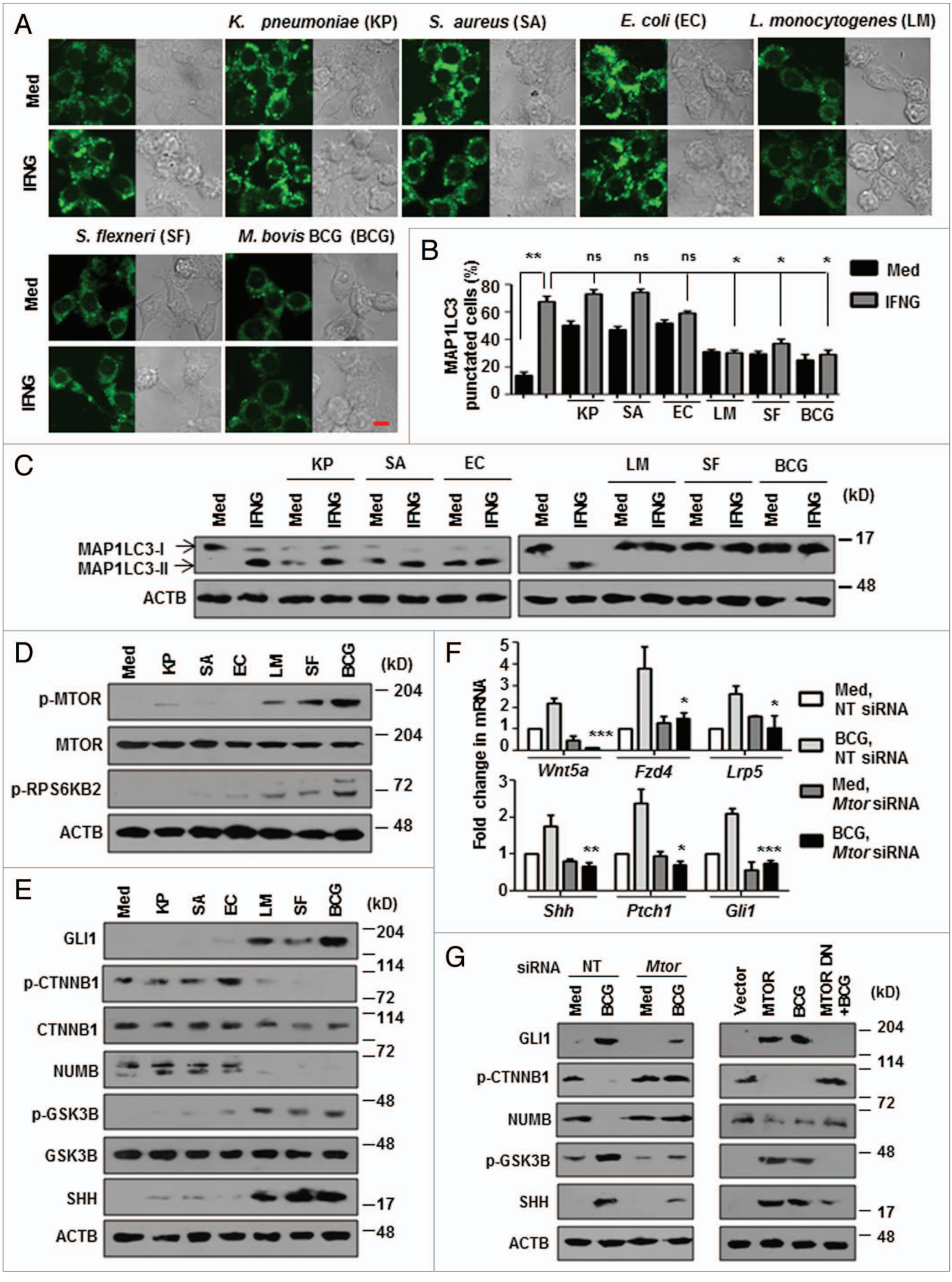

similar TLR2 dependency for MTOR activation (data not shown). Further, *M. bovis* BCG-infection of macrophages triggered marked activating phosphorylation of ULK1 (Ser555) while MTOR-dependent inhibitory phosphorylation of ULK1 (Ser757) was marginal (**Fig. S1E**). These data thus suggest that regulation of autophagy by mycobacteria via MTOR is ULK-independent. Therefore, we aimed at identifying other MTOR-responsive mediators that could play a role in abrogating IFNG-induced autophagy during mycobacterial infection.

Previously, we have demonstrated that TLR2-mediated signaling by *M. bovis* BCG triggers NOTCH,[18] WNT[19] and SHH[20] pathways in macrophages. Interestingly, MTOR can inhibit GSK3B,[31,32] a negative regulator of WNT and SHH pathways suggesting that WNT and SHH might be implicated in MTOR-dependent regulation of autophagy by *Mycobacteria* and other pathogens. In line with this hypothesis, *M. bovis* BCG, *S. flexneri,* and *L. monocytogenes* induced increased activation of both WNT and SHH pathways (**Fig. 1E**; **Fig. S1F**). WNT pathway activation was analyzed by transcript levels of WNT-responsive genes *Wnt5a*, *Fzd4*, and *Lrp5* and phosphorylation status of CTNNB1 and GSK3B. Phosphorylated CTNNB1 (Ser33 and Ser37, as well as Thr41) indicates inactivation of WNT pathway whereas phosphorylation at Ser9 renders GSK3B inactive and activates WNT signaling. Transcript analysis of *Shh*, *Ptch1*, and *Gli1* and protein level expression of SHH, GLI1, NUMB, GSK3B were utilized as read out for activation of canonical SHH signaling. Increased SHH, GLI1, p-GSK3B (Ser9) and decreased NUMB indicates active SHH signaling. MTOR-mediated activation of these pathways was further confirmed by the inability of *M. bovis* BCG to induce the activation WNT and SHH pathways in the presence of *Mtor*-specific siRNA or DN (**Fig. 1F and G**; **Fig. S1G**) and that overexpression of MTOR in macrophages induced WNT and SHH pathways (**Fig. 1G**; **Fig. S1G**).

We further corroborated the inhibitory effects of WNT and SHH signaling on IFNG-induced autophagy by overexpression and knockdown experiments. Ectopic expression of WNT5A and SHH proteins drastically abrogated IFNG-induced MAP1LC3 lipidation and puncta formation (**Fig. 2A and B**; **Fig. S2A and S2B**). Substantiating this observation, inhibition of WNT and SHH signaling either by pharmacological inhibitors or by RNA interference of *Wnt5a*, *Ctnnb1*, *Shh,* or *Gli1* significantly reduced the ability of *M. bovis* BCG to inhibit IFNG-induced autophagy (**Fig. 2C–F**; **Fig. S2C–S2F**).

GSK3B regulation by MTOR-PP2A influences autophagy

Protein phosphatases such as PP2A, a Ser/Thr protein phosphatase, have been implicated in the process of autophagy.[2] PP2A dephosphorylates the inactive GSK3B to active form.[33] However, the specificity of PP2A is attributed to the numerous regulatory subunits, among which, B56 (PPP2R5A)-containing PP2A has been proposed to have an inhibitory role on WNT[34-36] and SHH[37,38] pathways. As GSK3B inhibition was found to be MTOR-responsive (**Fig. 1G**), we investigated the repercussion of regulation of GSK3B by MTOR and PPP2R5A on autophagy. Interestingly, by RNA interference of either MTOR (*Mtor* siRNA) or individual molecular complexes (MTORC1-*Rptor* siRNA and MTORC2-*Rictor* siRNA), we found that *M. bovis* BCG downregulates the expression of PPP2R5A protein, but not transcripts, in an MTOR-dependent manner (**Fig. 3A and B**; **Fig. S2G and S2H**). Corroborating this result, both MTORC1 and MTORC2 seem to possess the ability to inhibit IFNG-induced autophagy, though the latter was comparatively less effective (**Fig. 3C**). Coimmunoprecipitation of PPP2R5A and GSK3B further confirmed the PP2A-GSK3B regulatory interactions (**Fig. 3D**). Importantly, macrophages that were transfected with *Ppp2r5a*-specific siRNA remained refractory to IFNG-triggered autophagy thus underscoring the importance of PPP2R5A in autophagy (**Fig. 3E and F**; **Fig. S2I**). In accordance, overexpression of PPP2R5A in macrophages strongly repressed *M. bovis* BCG-driven inhibitory effects on IFNG-induced autophagy (**Fig. 3G and H**; **Fig. S2J**) and failed to induce WNT and SHH pathway in response to *M. bovis* BCG (**Fig. 3I**). Together, these results demonstrate that pathogens could evade host response such as autophagy by modulating PP2A levels.

***Mir155* and *Mir31* target *Ppp2r5a* to limit autophagy**

M. bovis BCG-induced decrease in PPP2R5A protein but not the transcripts (**Fig. 3A and B**), strongly advocates a role for posttranscriptional regulatory mechanisms like those mediated by miRNAs. Data from a miRNA microarray[20] together with extensive bioinformatic analysis (TargetScan, miRanda, miRWalk and RNAhybrid) identified *Ppp2r5a* as a potential target for *Mir155* and *Mir31*. The target sites located at the residues spanning from 1022 to 1028 (for *Mir155*) and 960 to 967 (for *Mir31*) in *Ppp2r5a* mRNA were identified as critical for miRNA-3′UTR interactions (**Fig. 4A**).

To explore their possible role in the current study, macrophages infected with the panel of bacteria were analyzed for induced expression of *Mir155* and *Mir31*. Infection with

Figure 2 (See opposite page). WNT-SHH signaling contributes to *M. bovis* BCG-mediated inhibition of autophagy. (**A**) Cotransfection of RAW 264.7 macrophages with pEGFP-MAP1LC3 and WNT5A or SHH overexpression constructs were performed, treated with IFNG and number of cells expressing MAP1LC3 puncta were quantified. (**B**) Immunoblot analysis of MAP1LC3 cleavage state in murine RAW 264.7 cells transfected with WNT5A or SHH or both WNT5A and SHH overexpression constructs and treated with IFNG (200 U/ml) for 2 h. (**C and D**) Transient cotransfection of RAW 264.7 macrophages with pEGFP-MAP1LC3 and the indicated siRNA was performed and treated as indicated in (**A**). Representative immunofluorescence images are shown (**C**) and the number of cells expressing MAP1LC3 puncta was quantified (**D**). (**E**) Macrophages derived from peritoneal exudates of C3H/HeJ mice were pretreated with pharmacological inhibitors of the WNT signaling pathway like FH535 (CTNNB1/TCF inhibitor), IWP-2 (WNT secretion inhibitor) and the SHH signaling pathway like Cyclopamine (SMO inhibitor), Betulinic Acid (GLI inhibitor) for 1 h, infected with *M. bovis* BCG for 12 h and treated with IFNG for 2 h as indicated. Lysates were analyzed for MAP1LC3-I/-II patterns by immunoblotting. (**F**) Murine RAW 264.7 macrophages were transiently transfected with NT or indicated siRNA. 48 h post transfection, cells were infected with *M. bovis* BCG for 12 h, followed by 2 h treatment with IFNG. Immunoblot analysis for MAP1LC3 cleavage was performed. All data represent the mean ± SEM for 5 to 6 values from 3 independent experiments, $*P < 0.05$, $**P < 0.005$ (one-way ANOVA) and all blots are representative of 3 independent experiments. The cells were infected with bacteria at MOI 1:10 in the experiments. Med, medium; NT, nontargeting. Scale bar: 5 μm.

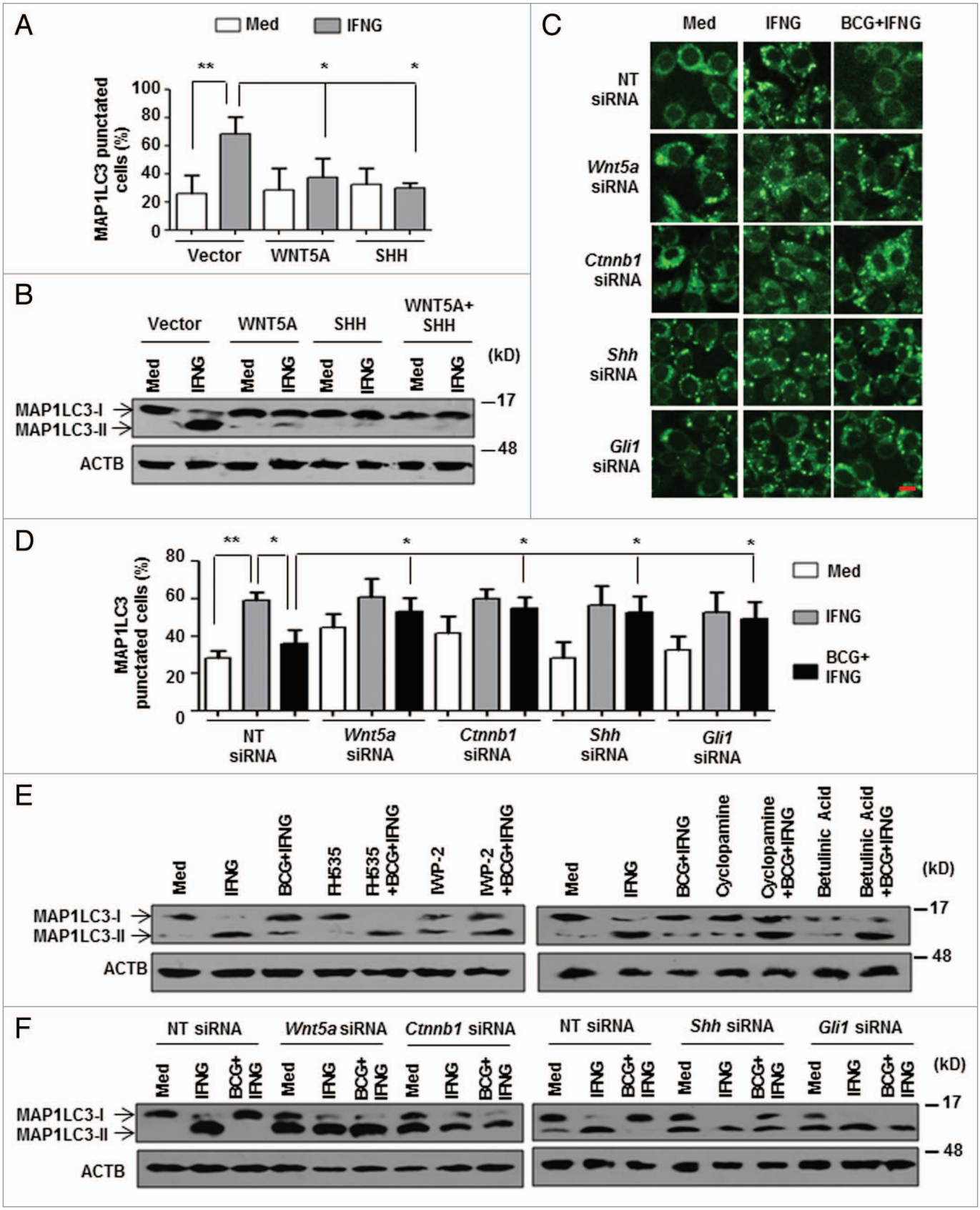

Figure 2. For figure legend, see page 314.

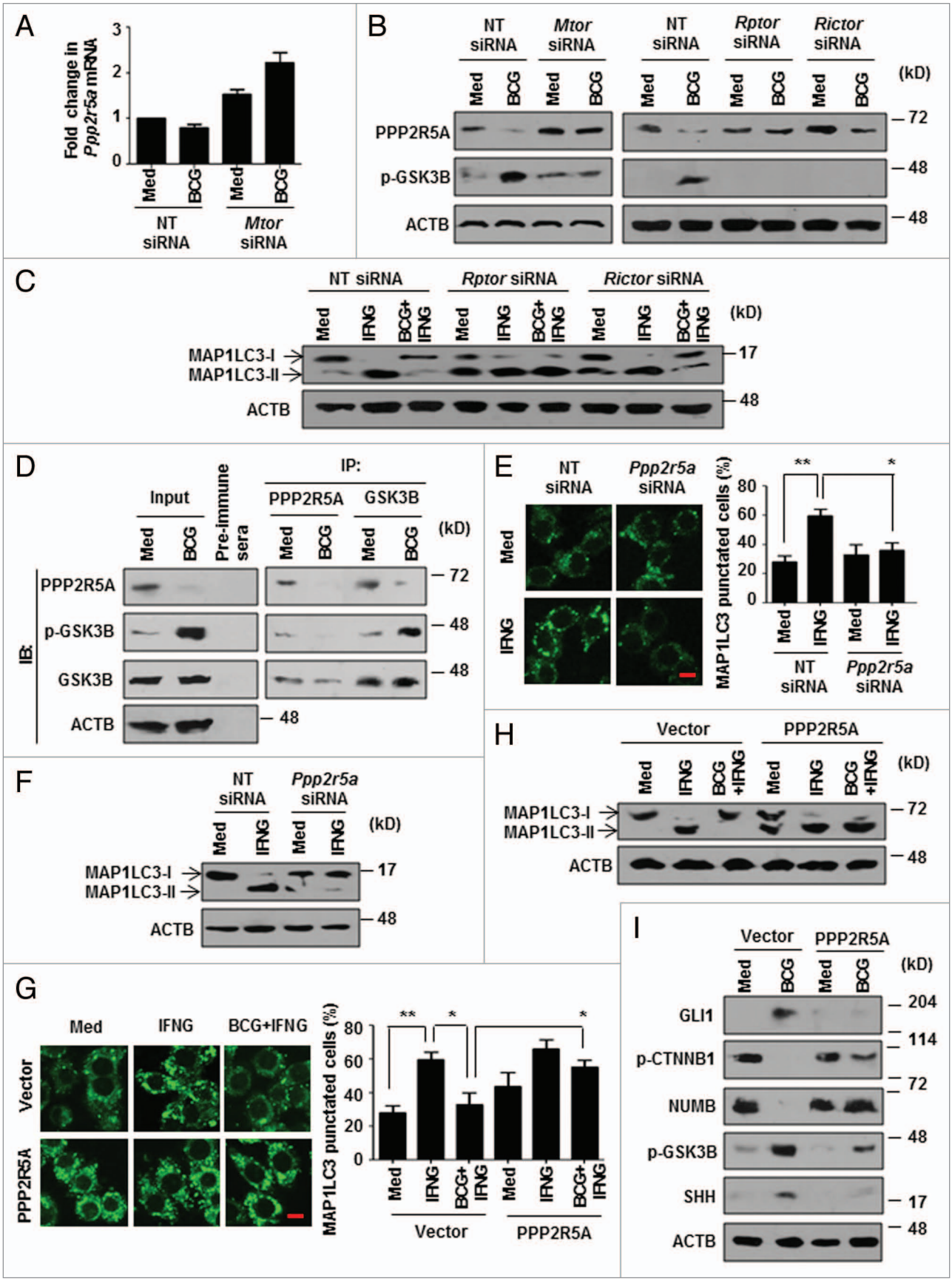

Figure 3. For figure legend, see page 317.

M. bovis BCG, *S. flexneri,* and *L. monocytogenes* but not with *K. pneumoniae*, *S. aureus,* and *E. coli* elicited robust expression of *Mir155* and *Mir31* (**Fig. 4B**). Importantly, *M. bovis* BCG infection or transfection with *Mir155* or *Mir31* mimics markedly reduced WT *Ppp2r5a* 3′UTR luciferase activity. However, the reduction was not significant when single mutants (for *Mir155* or *Mir31* binding sites) or double mutants (for *Mir155* and *Mir31* binding sites) *Ppp2r5a* 3′UTR constructs were utilized. Interestingly, *Mir155* or *Mir31* mutant reporters did exhibit a significant decrease in control experiments in presence of *Mir31* or *Mir155* mimics respectively (**Fig. 4C**). These results thus validate that *Ppp2r5a* is a direct target of *Mir155* and *Mir31*.

To further corroborate the direct interaction of *Ppp2r5a* with *Mir155* and *Mir31*, RNA immunoprecipitation of AGO2 (argonaute RISC catalytic component 2) was performed. As shown in **Figure 4D**, *Mir155*, *Mir31* and *Ppp2r5a* mRNA were significantly enriched in AGO2 immunoprecipitates in WT bone marrow-derived macrophages (BMDMs). However, enrichment of *Mir155* and *Ppp2r5a* mRNA in the AGO2 immunoprecipitates was severely reduced in *mir155*-deficient BMDMs. *Mir106a* was used as a nonspecific control that did not vary with *M. bovis* BCG infection. Together, these results suggest that *Ppp2r5a* is a bonafide target of *M. bovis* BCG-induced *Mir155* and *Mir31*.

In agreement with the above results, infection-induced *Mir155* and *Mir31* were found to be dependent on MTOR (**Fig. 4E**; **Fig. S3A**) and TLR2 (**Fig. S3B**). Upon *M. bovis* BCG infection of macrophages, MTOR-dependent increased H3K4me3 and decreased H3K27me3 methylations, that mark active transcription, were observed at the *Mir155* and *Mir31* promoters. (**Fig. 4F**). Interestingly, a previous investigation suggested a role for MTOR in modulating H3K4 methylations.[39] In this perspective, we speculated that MTOR mediates these epigenetic changes at *Mir155* and *Mir31* promoters by regulating the histone-modifying enzyme ASH2L, a component of the KMT2A/MLL-SETD1A/SET1 family of histone methyltransferases that mediates H3K4 methylation. Consistent with the H3K4me3 chromatin immunoprecipitation (ChIP) data, recruitment of ASH2L to the promoters of *Mir155* and *Mir31* was found to be MTOR-dependent as pharmacological inhibition of MTOR by rapamycin severely abrogated the *M. bovis* BCG-induced ASH2L recruitment to the *Mir155* and *Mir31* promoters (**Fig. 4F**).

Inhibition of PPP2R5A activity by *Mir155* and *Mir31* was further confirmed by evaluating the activation status of GSK3B. Upon *M. bovis* BCG infection, BMDMs from *mir155*-null mice as well as *Mir155* or *Mir31* siRNA-transfected macrophages failed to abrogate PPP2R5A levels resulting in decreased inactive GSK3B (p-GSK3B) (**Fig. 5A**). Concomitantly, enforced expression of *Mir155* and *Mir31* resulted in markedly reduced PPP2R5A levels and increased inactive form of GSK3B (**Fig. 5A**; **Fig. S3C**). Substantiating these results, we also observed that BMDMs from *mir155*-null mice or *Mir155* or *Mir31* siRNA-transfected macrophages were unable to activate *M. bovis* BCG-induced WNT and SHH signaling, whereas, *Mir155* or *Mir31* mimics alone could activate WNT and SHH signaling as indicated by the increased p-CTNNB1, p-GSK3B, SHH, GLI1, and decreased NUMB expression (**Fig. 5B**).

In order to further delineate the mechanism of *Mir155* and *Mir31*-mediated inhibition of autophagy, we performed conventional gain-of-function and loss-of-function analyses. Knockdown of *Mir155* and *Mir31* using specific siRNAs in macrophages significantly reduced the ability of *M. bovis* BCG to inhibit IFNG-induced autophagy as shown by MAP1LC3 puncta (**Fig. 5C**). MAP1LC3-II lipidation further confirmed the compromised ability of *M. bovis* BCG to inhibit autophagy in *Mir155* or *Mir31* siRNA-transfected macrophages as well as in *mir155*-deficient BMDMs (**Fig. 5D and E**). In agreement with these observations, *Mir155* or *Mir31* mimic-transfected macrophages could significantly reduce IFNG-induced autophagy (**Fig. 5F–H**). These results thus strongly implicate *Mir155* and *Mir31* in the modulation of PPP2R5A and downstream signaling pathways that regulate autophagy.

Mir155-Mir31-WNT-SHH arbitrate infection-induced ALOX

Pathogens such as mycobacteria successfully evade the host immune response by triggering antiinflammatory pathways.[40,41] ALOX/LO (arachidonate lipoxygenase)-mediated production of lipoxins (LXs), which are chalones in inflammatory responses, represents one such mechanism.[42,43] Therefore, we examined the expression of ALOXs such as ALOX5 and ALOX15 in response to the tested microbes. Notably, microbes that inhibited IFNG-induced autophagy, *M. bovis* BCG, *S. flexneri,* and *L. monocytogenes*, induced marked levels of both ALOX5 and ALOX15 (**Fig. 6A**; **Fig. S4A**). Further, by using macrophages from *tlr2*-null mice and macrophages transfected with *Mtor*

Figure 3 (See opposite page). MTOR-PP2A regulate GSK3B activity to modulate autophagy. (**A and B**) Quantitative real-time RT-PCR (**A**) and immunoblot analysis (**B**) for *Ppp2r5a* and PPP2R5A, p-GSK3B respectively from *M. bovis* BCG-infected murine RAW 264.7 macrophages transfected with NT or the indicated siRNA. (**C**) Transient transfection of RAW 264.7 macrophages with the indicated siRNA was performed, infected with *M. bovis* BCG for 12 h, followed by 2 h treatment with IFNG. Immunoblot analysis for MAP1LC3. (**D**) Anti-PPP2R5A and anti-GSK3B immunoprecipitations were performed with *M. bovis* BCG-infected C3H/HeJ peritoneal macrophages. The immunoprecipitates were subjected to immunoblotting using the indicated antibodies. (**E**) Murine RAW 264.7 macrophages were transiently transfected with pEGFP-MAP1LC3 and NT or *Ppp2r5a* siRNA, followed by IFNG (200 U/ml) treatment for 2 h. Representative immunofluorescence images are shown (left panel) and the number of cells expressing MAP1LC3 puncta was quantified (right panel). (**F**) Immunoblot analysis of MAP1LC3-I and II levels in IFNG-treated murine RAW 264.7 cells transfected with NT or *Ppp2r5a* siRNA. (**G**) Immunofluorescence assay was performed using pEGFP-MAP1LC3 and 3HA-PPP2R5A transfected RAW 264.7 macrophages infected with *M. bovis* BCG for 12 h and treated with IFNG for 2 h as indicated. Shown are the representative images (left panel) and the enumerated cells exhibiting MAP1LC3 puncta (right panel). (**H and I**) MAP1LC3 lipidation state and WNT-SHH signaling markers were determined in macrophages overexpressing 3HA-PPP2R5A with the indicated treatment by immunoblotting. All data represent the mean ± SEM for 5 to 6 values from 3 independent experiments, $^{*}P < 0.05$, $^{**}P < 0.005$ (one-way ANOVA) and all blots are representative of 3 independent experiments. The cells were infected with bacteria at MOI 1:10 in the experiments. Med, medium; NT, nontargeting; IP, immunoprecipitation; IB, immunoblotting. Scale bar: 5 μm.

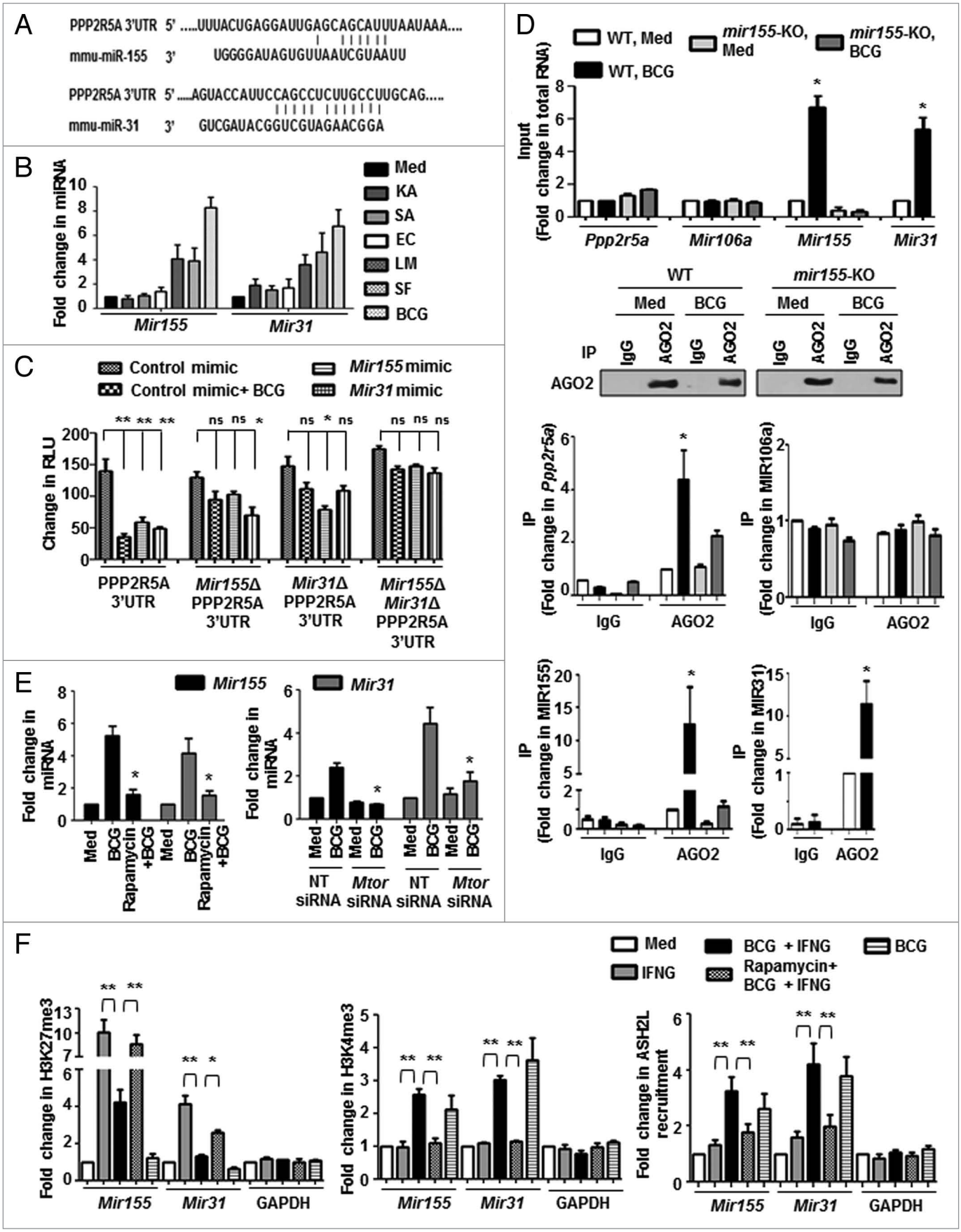

Figure 4. For figure legend, see page 319.

siRNA or the MTOR overexpression construct, we show that *M. bovis* BCG-mediated ALOX induction was TLR2- and MTOR-dependent (**Fig. 6B**; **Fig. S4B and S4C**).

We then explored molecular mechanisms that promote infection-induced ALOX expression. As *M. bovis* BCG infection induced robust expression of *Mir155* and *Mir31*, we investigated the role of these miRNAs in the regulation of ALOX. We show that *mir155*-null BMDMs or *Mir31* siRNA-transfected macrophages failed to induce ALOX5 and ALOX15 upon *M. bovis* BCG infection (**Fig. 6C and D**). In agreement with this, enforced expression of *Mir155* and *Mir31* augmented the expression of ALOX5 and ALOX15 (**Fig. 6D**). Also, PPP2R5A negatively regulated the expression of infection-induced ALOXs (**Fig. 6E**).

Next, contribution of induced WNT and SHH signaling pathways in driving ALOX expression was verified. Overexpression of WNT5A and SHH (**Fig. 6F and G**) in macrophages instigated the expression of ALOX5 and ALOX15 whereas pharmacological inhibition (**Fig. 6H**; S4D and S4E) or siRNA-mediated interference (**Fig. 6I**) of WNT and SHH signaling mediators (*Wnt5a*, *Ctnnb1*, *Shh*, or *Gli1)* significantly impaired the ability of *M. bovis* BCG to induce ALOXs. Finally, ChIP assays were performed to confirm the participation of TLR2-responsive WNT and SHH signaling effectors, CTNNB1 and GLI1 respectively, in regulating the expression of both ALOX5 and ALOX15. By using MatInspector program, a total of 8 and 5 CTNNB1 binding sites and 2 and 3 GLI binding sites were identified in promoters (2 kb upstream from the start site) of *Alox5* and *Alox15* genes respectively. Interestingly, TLR2-dependent 2- to 3-fold recruitment of CTNNB1 and GLI1 to the promoters of *Alox5* and *Alox15* was observed (**Fig. 6J**). Altogether, these results demonstrate that *Mir155-Mir31*-WNT-SHH arbitrate infection-induced ALOX expression in a TLR2-dependent manner.

ALOXs downregulate IFNG signaling to subdue autophagy

As *Mir155-Mir31*-WNT-SHH coordinated the *M. bovis* BCG-induced ALOXs, it raised the possibility that ALOXs play a critical role in autophagy. Accordingly, knockdown of ALOXs using specific siRNA (**Fig. 7A–D**) or utilization of ALOXs-specific pharmacological inhibitors (**Fig. 7E and F**) significantly repressed the ability of *M. bovis* BCG to inhibit IFNG-induced autophagy. Conversely, macrophages overexpressing ALOX5 or ALOX15 reduced the IFNG-induced autophagy (**Fig. 7G and H**).

IFNG activates the downstream STAT1 (signal transducer and activator of transcription 1) signaling to induce antimicrobial activity of macrophages such as autophagy.[44] In this regard, we examined the effect of ALOXs on the IFNG-induced STAT pathway. Suppression of JAK (janus kinase)-STAT signaling using pharmacological inhibitor AG490 severely compromised IFNG-induced autophagy (**Fig. 7I and J**). Interestingly, enforced expression of ALOX5 and ALOX15 significantly reduced the IFNG-mediated activation of STAT signaling (**Fig. 7K**).

In addition to *M. bovis* BCG, virulent *M. tuberculosis* also exhibited the ability to inhibit IFNG-induced autophagy by arbitrating the infection-induced ALOX expression via induction of *Mir155-Mir31*-WNT-SHH signaling (**Fig. 8**). Further, to analyze the functional consequence of altered IFNG-dependent autophagy in terms of bacterial replication, we performed intracellular CFU-based analysis of *M. bovis* BCG, *S. flexneri,* and *L. monocytogenes* in presence of inhibitors of the proposed pathway. As illustrated in **Figure 9A**, pharmacological perturbations of WNT (FH535), SHH (Cyclopamine), ALOX5 (AA-861), ALOX15 (PD146176) or MTOR (rapamycin) significantly reduced the ability of tested bacteria to resist IFNG-mediated bacterial clearance.

Discussion

Autophagy is one of the major host effector mechanisms to clear intracellular microbes. However, pathogens utilize several pathways to evade autophagy although microbes display differential abilities to counter autophagy.[10] In the present study, by using a panel of bacterial species, we elucidated the rationale and molecular signatures involved in autophagic evasion. We show that *M. bovis* BCG, *S. flexneri,* and *L. monocytogenes* but not *K. pneumoniae*, *S. aureus,* and *E. coli* inhibit IFNG-induced autophagy of macrophages via MTOR by *Mir155*- and *Mir31*-responsive WNT and SHH signaling. Though certain reports suggest the refractoriness of mycobacteria-infected macrophages toward IFNG,[18,45-51] we present molecular evidence that demonstrates repression of IFNG-induced JAK-STAT pathway during autophagy. Supporting our observation, previous reports suggest that *Mycobacteria* and its cell wall components, like TDM, downregulate IFNG-mediated responses by inhibiting STAT phosphorylation including p-STAT1.[52-54] Of note, individuals with STAT1 deficiency or defects in IFN-JAK-STAT pathway exhibit increased susceptibility to mycobacterial infections.[55,56] Impaired activation of STAT1 or reduced STAT1 phosphorylation in patients with active tuberculosis further underscores our data.[57,58]

Figure 4 (See opposite page). MTOR-responsive *Mir155* and *Mir31* target *Ppp2r5a*. (**A**) Putative *Mir155* and *Mir31* binding sites in the 3′UTR of *Ppp2r5a*. (**B**) Peritoneal macrophages from C3H/HeJ mice were infected with the indicated bacteria for 12 h and quantitative real-time RT-PCR analysis was performed on total RNA isolated using *Mir155* and *Mir31*-specific primers. (**C**) RAW 264.7 cells were transfected with WT or single mutant (*Mir155*Δ or *Mir31*Δ) or double mutant (*Mir155*Δ and *Mir31*Δ) *Ppp2r5a* 3′UTR luciferase construct with *Mir155* or *Mir31* mimics as indicated. 48 h post-transfection, cells were infected with *M. bovis* BCG as shown and luciferase assay was performed. (**D**) AGO2 immunoprecipitates from WT and *mir155*-null BMDMs were analyzed for enrichment of *Ppp2r5a*, MIR106a, *Mir155* and *Mir31* using quantitative real-time RT-PCR. Panel shows immunoprecipitated AGO2 using immunoblotting and immunoprecipitation with mouse IgG used as negative control. MIR106a was used as a nonspecific control. (**E**) Peritoneal macrophages from C3H/HeJ mice pretreated with Rapamycin (MTOR inhibitor) (left panel) or RAW 264.7 macrophages transfected with *Mtor* siRNA (right panel) were infected with *M. bovis* BCG for 12 h to assay the levels of *Mir155* and *Mir31* using quantitative real-time RT-PCR. (**F**) Peritoneal macrophages from C3H/HeJ were treated as indicated and H3K27me3 and H3K4me3 modifications, ASH2L recruitment at mouse *Mir155* and *Mir31* promoters were evaluated by ChIP. GAPDH promoter was analyzed as a control. All data represent the mean ± SEM for 5 to 6 values from 3 independent experiments, ns = not significant, **P* < 0.05, ***P* < 0.005 (one-way ANOVA) and all blots are representative of 3 independent experiments. The cells were infected with bacteria at MOI 1:10 in the experiments. Med, medium; NT, nontargeting; WT, wild-type; KO, knockout. Scale bar: 5 μm.

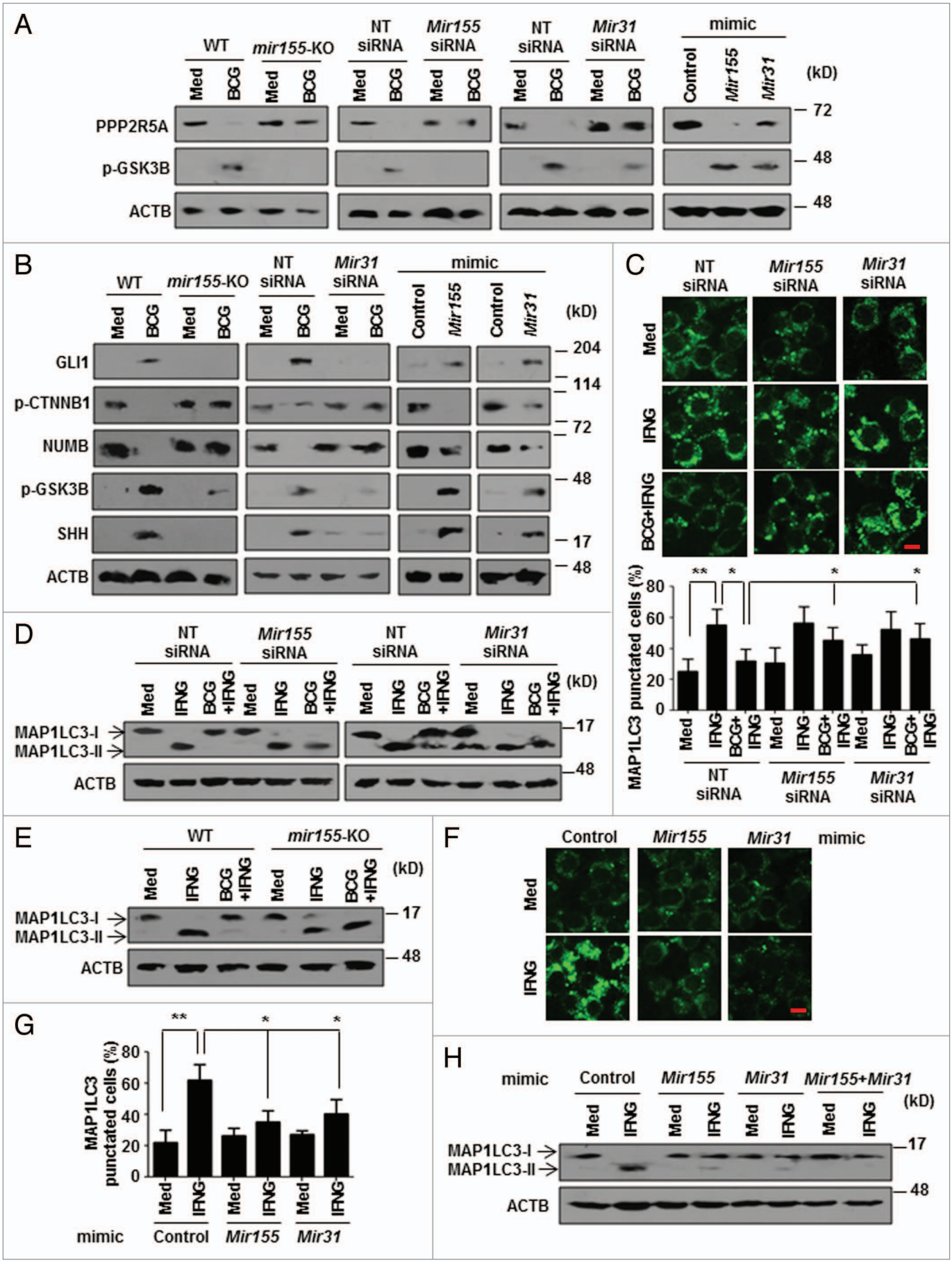

Interestingly, in the current study, both MTORC1 and MTORC2 contributed to the mycobacteria-mediated inhibition of IFNG-induced autophagy. This could be attributed to either the feed-forward loop from MTORC2 to MTORC1 or presence of MTORC2-dependent inhibitory effects on autophagy.[59]

The decisive role for TLR2 in shaping the outcome of infection with several pathogens, including mycobacteria, is well established.[20,60-62] However, contribution of TLR2 responses in modulating autophagy has not been addressed. Present observations could add new insights to the infection-induced TLR2 signaling during inhibition of autophagy. Interestingly, in agreement with our results, ligand-dependent activation of TLR4, as well as TLR7 and TLR8 but not TLR2 induces autophagy.[17] However, other TLR2 ligands like Pam3CSK4 or PIM2 failed to abrogate IFNG-induced autophagy when compared with *M. bovis* BCG (**Fig. S5A and S5B**). We would like to emphasize that whole viable mycobacteria do exhibit various immune evasion mechanisms including inhibition of IFNG responses by utilizing a complex network of signaling events. However, in our view, treatment with purified, TLR2 ligands may not reflect the infection scenario. Likewise, crucial signaling pathway determinants have been implicated to regulate autophagy. Recently, studies in *Drosophila* and mammalian cells have identified HH signaling to inhibit autophagy.[22] Herein, along with SHH signaling, our results attribute novel role for TLR2-dependent WNT signaling pathways in suppressing autophagy.

Post-transcriptional regulation of gene expression by miRNAs is fundamental for regulation of signaling pathways and consequently for calibrating the immune responses.[63,64] In the current context, *Mir155* and *Mir31* activate WNT-SHH pathway by targeting PP2A, a Ser/Thr phosphatase that determines GSK3B activity. We propose that infection-responsive, miRNA-mediated augmentation of WNT and SHH pathways are necessary for the sustained and long-term inhibition of autophagy of host cells that are constantly influenced by the dynamic cytokine milieu in vivo. In support of our proposition, B56-containing PP2A are implicated in the regulation of WNT and HH signaling in various cellular contexts.[34-38] Notably, pharmacological perturbation of PP2A inhibits autophagy in rat hepatocytes[2] and MTOR possesses inhibitory effects on PP2A.[65,66] We have previously demonstrated that *Mir155* induces apoptosis during *M. bovis* BCG infection of macrophages.[60] Apoptosis of the pathogen-infected cell, in general, is assumed to help cross-priming and thus activation of adaptive immune response. However, *Mycobacteria*-mediated apoptosis of the macrophages is known to assist in dissemination of the bacteria and thus act as a means for bacterial replication.[67] Fitting well into the known concepts of interplay between autophagy and apoptosis,[68] our data suggest that *M. bovis* BCG induces *Mir155* to inhibit autophagy and meanwhile promote macrophage apoptosis. Interestingly, activation of calpain during apoptosis could induce the cleavage of ATG5 and thus lead to inhibition of autophagy.[69] However, in the current study, inhibition of IFNG-induced autophagy by *M. bovis* BCG was significant even in the presence of ALLN, a calpain inhibitor and Z-VAD, a broad-spectrum caspase inhibitor ruling out such possibilities (**Fig. S6A–S6C**). Further, corroborating these results, *Mir155*-transfected macrophages markedly reduced IFNG-induced autophagy in presence of ALLN and Z-VAD (**Fig. S6D and S6E**). This suggests that *Mir155*-mediated apoptosis may not contribute to inhibition of autophagy in case of macrophages infected with *M. bovis* BCG. Previously, we have shown that SHH-responsive *Mir31* acts as a negative regulator of TLR2 responses to mycobacteria.[20] However, current evidence has identified a novel function of *Mir31* to inhibit autophagy by inducing SHH signaling, thus highlighting the ability of individual miRNAs to affect the expression of many proteins that could even constitute the same pathway.[70] Thus, our data advocates novel functions for *Mir155* and *Mir31* during the immune response to pathogens.

ALOXs play a significant role in determining the outcome of ensued immunity during infection. ALOXs inhibit Th1 cytokines and promote Th2 responses. Of note, ALOXs are targeted by many pathogens to evade immune surveillance.[71,72] A report also suggests that *alox5*-deficient mice are less prone to mycobacterial infections and exhibit rapid clearance of pathogens from the lungs.[73] We observed an indispensable role for the infection-induced ALOX5 and ALOX15 in controlling IFNG-induced autophagy. Albeit the precise mechanism involved in ALOX-LX-mediated inhibition of autophagy requires further study, we found that ALOXs mediate the downregulation of JAK-STAT signaling. STAT1-induced cytokine signaling in macrophages induces antibacterial effects including autophagy.[44] Interestingly, infection of macrophages with *M. bovis* BCG induces the expression of many inhibitors

Figure 5 (See opposite page). *M. bovis* BCG-induced *Mir155* and *Mir31* are requisite to activate WNT-SHH pathway and regulate autophagy. (**A and B**) Immunoblotting was performed to analyze the expression of PPP2R5A and p-GSK3B (**A**) or WNT-SHH pathway (**B**) on *M. bovis* BCG infection of BMDMs from *mir155*-null or WT mice or murine RAW 264.7 cells that were transiently transfected with *Mir155* or *Mir31* siRNAs or *Mir155* or *Mir31* mimic. (**C**) Knockdown of *Mir155* and *Mir31* was achieved by transfecting specific siRNAs in RAW 264.7 macrophages. 48 h post-transfection, macrophages were infected with *M. bovis* BCG for 12 h followed by IFNG (200 U/ml) treatment for 2 h. Representative immunofluorescence images are shown (top panel) and the number of cells expressing MAP1LC3 puncta was quantified (bottom panel). (**D**) Murine RAW 264.7 macrophages were transiently transfected with *Mir155* or *Mir31* siRNA, *M. bovis* BCG infected for 12 h and treated with IFNG for 2 h. Immunoblots for MAP1LC3 cleavage state. (**E**) BMDMs from *mir155*-null mice or WT mice were infected with *M. bovis* BCG and the total cell lysate was analyzed for MAP1LC3-I/-II levels by immunoblotting. (**F-H**) Experiments were performed with pEGFP-MAP1LC3 (**F and G**) or without pEGFP-MAP1LC3 (**H**). *Mir155* or/and *Mir31* mimic transfected RAW 264.7 macrophages were treated with IFNG for 2 h as indicated. Shown in (**F**) are the representative immunofluorescence images, (**G**) shows the enumerated cells exhibiting MAP1LC3 puncta and (**H**) shows immunoblotting for MAP1LC3-I/-II. Macrophages in (**H**) were transfected with 25 nM *Mir155* and *Mir31*. All data represent the mean ± SEM for 5 to 6 values from 3 independent experiments, $^{*}P < 0.05$, $^{**}P < 0.005$ (one-way ANOVA) and all blots are representative of 3 independent experiments. The cells were infected with bacteria at MOI 1:10 in the experiments. Med, medium; NT, nontargeting; WT, wild-type; KO, knockout. Scale bar: 5 μm.

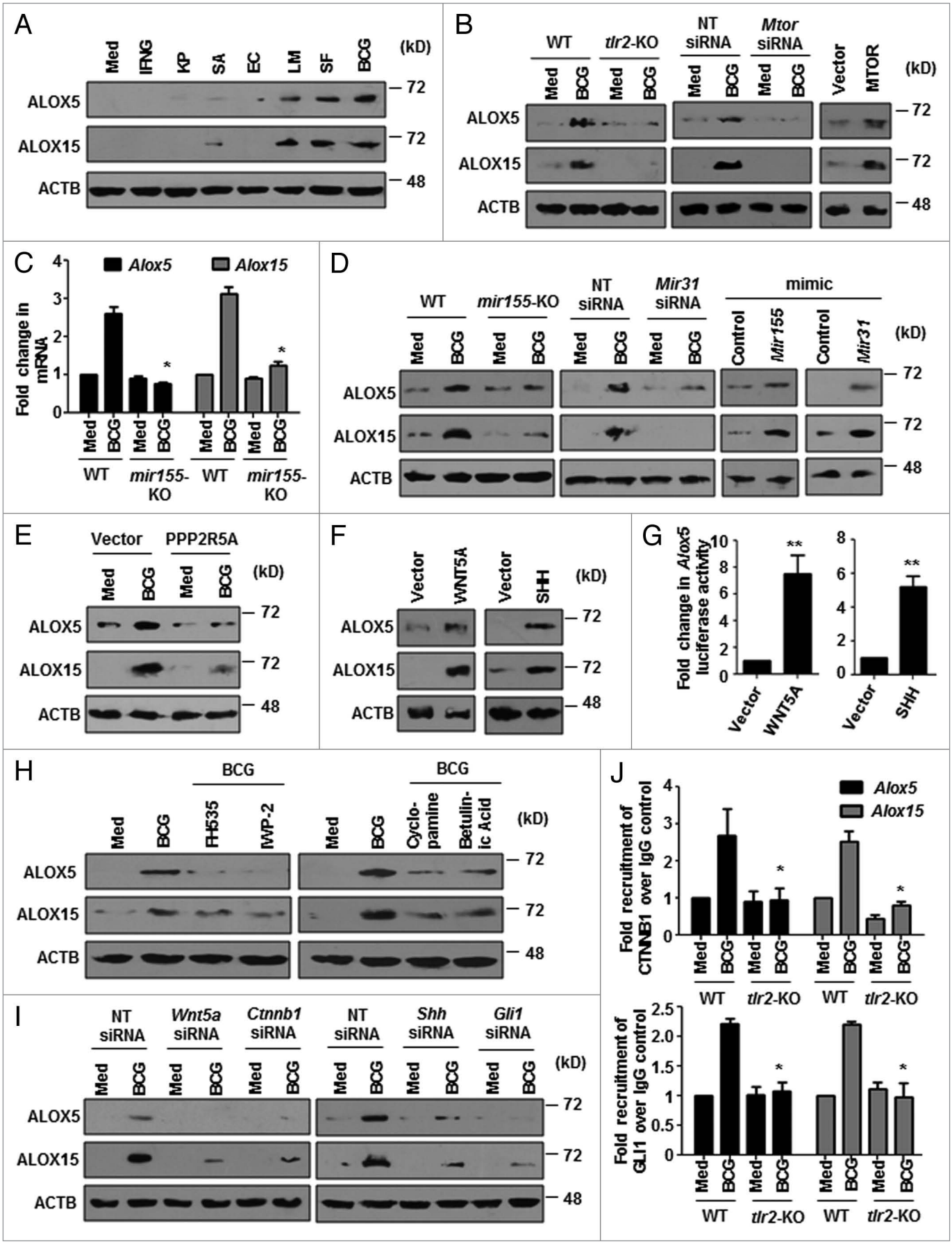

of cytokine signaling such as SOCS and PIAS, which may support the current observations.[18,74,75] Alternatively, ALOX-LX signaling might activate PI3Ks,[76] veritable inhibitors of autophagy.

Interestingly, similar to *M. bovis* BCG-induced responses, we found that virulent *M. tuberculosis* could inhibit IFNG-induced autophagy via the MTOR-*Mir155-Mir31*-WNT-SHH-ALOX pathway. However, *M. tuberculosis*-mediated inhibition was less effective when compared with *M. bovis* BCG. These results are in agreement with the recent reports, which suggest that *M. tuberculosis* can inhibit autophagy.[13,16,77]

In summary, our results have implicated multiple host factors such as *Mir155-Mir31* and WNT-SHH-ALOXs to orchestrate the microbe-induced evasion of autophagy (**Fig. 9B**). These molecular regulators bear potential importance in disease control by aiding the search for effective drugs and therapeutics.

Material and Methods

Cells, mice, and bacteria

Primary macrophages were isolated from peritoneal exudates of C57BL/6J (000664), C3H/HeJ (000659) and *tlr2*-KO (004650) mice that were purchased from The Jackson Laboratory and maintained in the Central Animal Facility, Indian Institute of Science. Briefly, mice were intraperitoneally injected with 1 ml of 8% Brewer thioglycollate. After 4 d of injection, mice were sacrificed and peritoneal cells were harvested by lavage from peritoneal cavity with ice-cold PBS. The cells were cultured in DMEM (Gibco-Invitrogen, 12100-061) containing 10% FBS (Gibco-Invitrogen, 10270-106) for 6 to 8 h and adherent cells were used as peritoneal macrophages. All studies involving mice were performed after the approval from the Institutional Ethics Committee for animal experimentation as well as from Institutional Biosafety Committee. *mir155*-KO mice and littermate controls were generated as described earlier.[78,79] BMDMs were isolated from femurs and tibias obtained from WT or *mir155*-KO mice and cultured in DMEM medium containing 30% L-929 fibroblast-conditioned medium for 7 d. The purity of these cells was confirmed by F4/80 staining using FACS and was > 95%. All transfection studies were performed in murine RAW 264.7 macrophage-like cells obtained from the National Center for Cell Sciences, Pune, India. *M. bovis* BCG Pasteur 1173P2 was obtained from Pasteur Institute, Paris, France and *S. aureus, K. pneumoniae, S. flexneri, L. monocytogenes*, and *E. coli* were obtained from The Microbial Type Culture Collection and Gene Bank (MTCC), Chandigarh, India. Bacteria were grown to mid-log phase and used at 10 multiplicity of infection (MOI) in all the experiments unless mentioned otherwise.

Reagents and antibodies

General laboratory chemicals were obtained from Sigma-Aldrich or Merck. IFNG was purchased from PeproTech Inc. (315-05). Anti-ACTB (A3854) and anti-AGO2 (SAB4200085) antibodies was purchased from Sigma-Aldrich. Anti-MAP1LC3I/II (4108), anti-Ser-33/37/Thr-41 phospho CTNNB1 (9561), anti-CTNNB1 (9562), anti-WNT5A (2392), anti-SHH (2207), anti-GLI1 (2534), anti-NUMB (2756), anti-Ser9 phospho GSK3B (9322), anti- GSK3B (5195), anti-ALOX5 (3289), anti-Ser2448 phospho MTOR (2971), anti-MTOR (2972), anti-Thr389 phospho RPS6KB2 (9205), anti-Thr37/46 phospho EIF4EBP1 (9455), anti-RPTOR (2280), anti-RICTOR (2114), anti-Ser555 phospho ULK1 (5869), anti-Ser757 phospho ULK1 (6888), anti-H3K27me3 (9733), anti-H3K4me3 (9751), anti-ASH2L (5019), anti-Tyr705 phospho STAT3 (9131) and anti-Tyr701 phospho STAT1 (9171) were purchased from Cell Signaling Technology. Anti-PPP2R5A (sc-136045) and anti-ALOX15 (sc-32940) were purchased from Santa Cruz Biotechnology, Inc. HRP conjugated anti-rabbit IgG (111-035-045) and anti-mouse IgG (115-001-003) were obtained from Jackson ImmunoResearch.

Treatment with pharmacological reagents

In all experiments, cells were treated with the given inhibitor for 1 h before experimental treatments at the following concentrations: Rapamycin (100 nM) (Calbiochem, 553210), FH535 CTNNB1 and TCF (transcription factor family) inhibtor (15 μM) (Calbiochem, 219330), IWP-2 (5 μM) (Calbiochem, 681671), cyclopamine (10 μM) (Calbiochem, 239803), betulinic Acid (10 μM) (Calbiochem, 200498), AA-861 (10 μM) (Sigma-Aldrich, A3711), PD146176 (10 μM) (Sigma-Aldrich, P4620), AG490 (10 μM) (Calbiochem, 658401), manumycin A (10 μM) (Calbiochem, 444170), propranolol (10 μM) (Calbiochem, 537075), LY294002 (50 μM)

Figure 6 (See opposite page). *Mir155*- and *Mir31*-regulated WNT-SHH induce expression of ALOXs. (**A**) Peritoneal macrophages from C3H/HeJ mice were infected with the indicated microbes for 12 h or treated with IFNG for 2 h and immunoblotting was performed to analyze expression of ALOX5 and ALOX15. (**B**) Macrophages derived from WT or *tlr2*-null mice (left panel) or murine RAW 264.7 cells transfected with NT or *Mtor* siRNA (middle panel) were infected with *M. bovis* BCG for 12 h or MTOR was ectopically expressed in macrophages by transfection with pcDNA3-MTOR plasmid (right panel) and the total cell lysates were probed for ALOX5 and ALOX15 by immunoblotting. (**C**) Quantitative real-time RT-PCR for *Alox5* and *Alox15* in *M. bovis* BCG infected BMDMs obtained from WT or *mir155*-null mice. (**D and E**) Immunoblotting was performed with specific antibodies to ALOX5 and ALOX15 under different experimental setups; BMDMs from *mir155*-null mice or WT mice, macrophages that were transiently transfected *Mir31* siRNA, control or *Mir155* or *Mir31* mimic transfected RAW 264.7 macrophages (**D**), macrophages transfected with 3HA-PPP2R5A overexpression construct (**E**), were infected with *M. bovis* BCG for 12 h as indicated. (**F and G**) Ectopic expression of WNT5A or SHH in macrophages was performed and analyzed for ALOX5 and ALOX15 by immunoblotting (**F**) and *Alox5* promoter activity by luciferase assay (**G**). (**H**) Peritoneal macrophages from C3H/HeJ mice were pretreated with pharmacological inhibitors of the WNT signaling pathway like FH535 (CTNNB1/TCF inhibitor), IWP-2 (WNT secretion inhibitor) and the SHH signaling pathway like Cyclopamine (SMO inhibitor), Betulinic Acid (GLI inhibitor) for 1 h, infected with *M. bovis* BCG for 12 h and immunoblotting was performed to determine the expression of ALOX5 and ALOX15. (**I**) RAW 264.7 macrophages harboring specific siRNA to silence WNT and SHH pathways were utilized for assessing ALOX5 and ALOX15 protein levels on *M. bovis* BCG infection. (**J**) The recruitment of CTNNB1 and GLI1 at mouse *Alox5* and *Alox15* promoters upon infection with *M. bovis* BCG in wild type and *tlr2*-null macrophages was evaluated by ChIP assay. All data represent the mean ± SEM for 5 to 6 values from 3 independent experiments, $*P < 0.05$ (one-way ANOVA in I), $**P < 0.005$ (*t* test in G) and all blots are representative of 3 independent experiments. The cells were infected with bacteria at MOI 1:10 in the experiments. Med, medium; NT, nontargeting; WT, wild-type; KO, knockout.

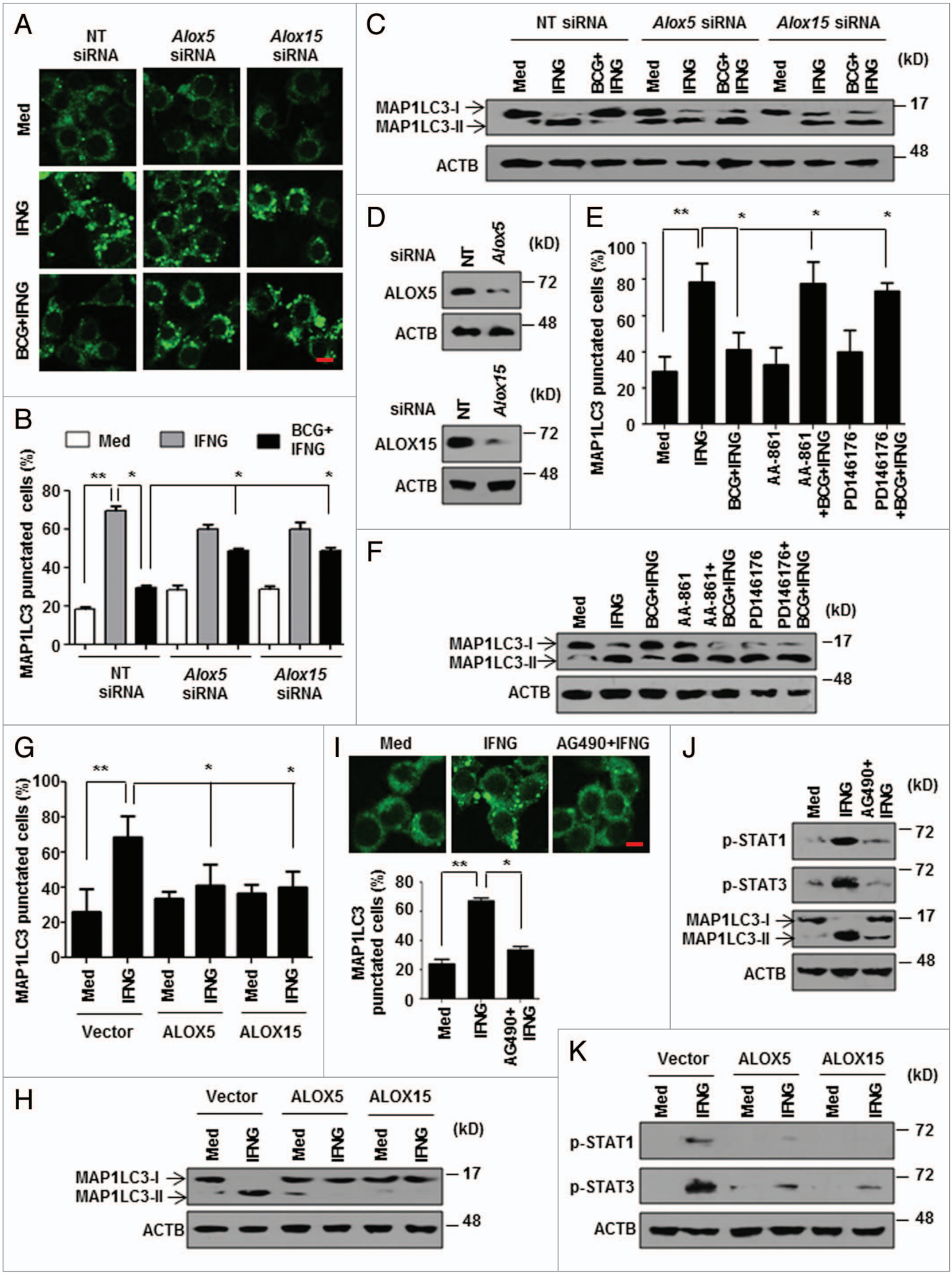

(Calbiochem, 440202), ALLN, calpain inhibitor I (10 μM) (Sigma, A6185) and Z-VAD (20 μM) (Calbiochem, 620610). DMSO at 0.1% concentration was used as the vehicle control. In all experiments involving pharmacological reagents, a tested concentration was used after careful titration experiments assessing the viability of the macrophages using the MTT (3-(4,5-Dimethylthiazol-2-yl)-2,5-diphenyltetrazolium bromide) assay. Pam3CSK4 (1 μg/ml) (Imgenex, IMG 2201) and PIM2 (4 μg/ml) (Colorado State University) were also used.

***Ppp2r5a* 3′UTR WT and mutant generation**

The full-length 3′UTR of *Ppp2r5a* was PCR amplified and cloned into a pmirGLO vector using the restriction enzyme pair SacI and XbaI. The *Mir155* or *Mir31* binding sites in the 3′UTR of *Ppp2r5a* were mutated by nucleotide replacements through site-directed mutagenesis using the megaprimer inverse PCR method. The forward/reverse primer comprised the desired mutation and respective reverse primers were used to generate the megaprimer (listed in **Table S1**). The megaprimer was in turn used to amplify the miRGLO *Ppp2r5a* plasmid and generate the *Mir155*Δ and *Mir31*Δ 3′UTR mutants. The double mutant plasmid was generated utilizing a megaprimer mutant for *Mir31*-binding sites on the *Mir155*Δ mutant *Ppp2r5a* plasmid background.

Transfection studies

Murine RAW 264.7 macrophage cells were transfected with 5 μg of pEGFP-LC3 using low m.w. polyethylenimine (Sigma-Aldrich, 40872-7) in all the experiments involving immunofluorescence. Transiently transfection of RAW 264.7 macrophages with dominant negative (DN) mutant forms of TLR2 and MTOR or overexpression constructs of MTOR, WNT5A, SHH, PPP2R5A, ALOX5, ALOX15, WT *Ppp2r5a* 3′UTR, *Mir155*Δ *Ppp2r5a* 3′UTR, *Mir31*Δ *Ppp2r5a* 3′UTR, *Mir155*Δ *Mir31*Δ *Ppp2r5a* 3′UTR, β-Galactosidase (GLB1) was performed using low m.w. polyethylenimine. In case of experiments involving siRNA and mimics, RAW 264.7 macrophage cells were transfected with 100 nM siRNA or miRNA mimic unless mentioned otherwise. *Mtor* (M-065427-00), *Wnt5a* (M-065584-00), *Ctnnb1* (M-040628-00), *Shh* (M-042008-01), *Gli1* (M-047917-01), *Ppp2r5a* (M-040213-00), *Alox5* (M-065427-00), *Alox15* (M-061509-01), *Rptor* (M-058754-01), *Rictor* (M-064598-01), nontargeting siRNA (D-001210-01-20) and siGLO Lamin A/C (D-001620-03-05) were obtained from Dharmacon as siGENOME™ SMARTpool reagents, which contain a pool of four different double-stranded RNA oligonucleotides. *Mir155* (C-310430-07), *Mir31* (C-300507-05) and control mimics (CN-001000-01-05) were purchased from Dharmacon and *Mir155* and *Mir31* siRNAs (4390771) and control siRNA (4611G) were purchased from Ambion. Transfection efficiency was more than 50% in all the experiments as determined by counting the number of siGLO Lamin A/C positive cells in a microscopic field using fluorescent microscope. In all cases, 48 h post-transfection, the cells were treated or infected as indicated and processed for analysis.

Immunofluorescence

RAW 264.7 macrophages were seeded on to coverslips and treated as indicated. The cells were fixed with 3.7% paraformaldehyde for 15 min at room temperature and the coverslips were mounted on a slide with glycerol. Confocal images were taken on a Zeiss LSM 710 Meta confocal laser scanning microscope (Carl Zeiss AG) using a plan-Apochromat 63×/1.4 Oil DIC objective (Carl Zeiss AG) and images were analyzed using ZEN 2009 software.

RNA isolation and quantitative real-time RT-PCR

Macrophages were treated or infected as indicated and total RNA from macrophages was isolated by TRI reagent (Sigma-Aldrich, T9424). Two micrograms of total RNA was converted into cDNA using a First Strand cDNA synthesis kit (Bioline, BIO-65050). Quantitative real-time RT-PCR was performed using SYBR Green PCR mixture (KAPA Biosystems, KM4101) for quantification of the target gene expression. All the experiments were repeated at least 3 times independently to ensure the reproducibility of the results. *Gapdh* was used as internal control. The primers used for quantitative real-time RT-PCR amplification are summarized in **Table S1**.

Quantification of miRNA expression

For detection of *Mir155* and *Mir31*, total RNA was isolated from infected or treated macrophages using the TRI reagent. Quantitative real-time RT-PCR for *Mir155* (assay ID 002571), *Mir31* (assay ID 000185) and MIR106a (assay ID 002459) was performed using TaqMan miRNA assays (Life Technologies, 4427975) as per manufacturer's instructions. U6 snRNA was used for normalization.

Figure 7 (See opposite page). ALOXs dampen IFNG signaling to inhibit autophagy. (**A–C**) Knockdown of *Alox5* and *Alox15* was achieved by transfecting specific siRNAs in RAW 264.7 macrophages. 48 h post transfection, macrophages were infected with *M. bovis* BCG for 12 h followed by IFNG treatment for 2 h. pEGFP-MAP1LC3 was cotransfected in (**A and B**). Representative immunofluorescence images (**A**), enumeration of MAP1LC3 puncta (**B**) and immunoblot for MAP1LC3-I/-II (**C**) is shown. (**D**) Confirmation for siRNA-mediated knockdown of *Alox5* and *Alox15* after 12 h *M. bovis* BCG treatment. (**E**) Murine RAW 264.7 macrophages were transiently transfected with pEGFP-MAP1LC3, pretreated with pharmacological inhibitors of ALOX5 (AA-861) and ALOX15 (PD146176) for 1 h, infected with *M. bovis* BCG for 12 h and treated with IFNG for 2 h. Number of cells expressing MAP1LC3 puncta were quantified. (**F**) Peritoneal macrophages from C3H/HeJ mice were treated similar to (**E**). MAP1LC3 lipidation state was analyzed by immunoblotting. (**G and H**) Murine RAW 264.7 macrophages were transfected with ALOX5 and ALOX15 overexpression constructs and MAP1LC3 puncta were counted by immunofluorescence (**G**) and MAP1LC3 cleavage state was accessed by immunoblotting (**H**). pEGFP-MAP1LC3 was cotransfected in (**G**). (**I**) pEGFP-MAP1LC3 transfected murine RAW 264.7 macrophages were pretreated with AG490 (JAK2 inhibitor), infected with *M. bovis* BCG for 12 h followed by 2 h IFNG treatment. Representative immunofluorescence images are shown (top panel) and the number of cells expressing MAP1LC3 puncta was quantified (bottom panel). (**J**) Immunoblot for analysis of p-STAT1, p-STAT3 and MAP1LC3 lipidation using lysates obtained from peritoneal macrophages (from C3H/HeJ mice) treated as same in (**I**). (**K**) ALOX5 and ALOX15 were overexpressed in murine RAW 264.7 cells and assessed for phosphorylated forms of STAT1 and STAT3 using specific antibodies. All data represent the mean ± SEM for 5 to 6 values from 3 independent experiments, $^{*}P < 0.05$, $^{**}P < 0.005$ (one-way ANOVA) and all blots are representative of 3 independent experiments. The cells were infected with bacteria at MOI 1:10 in the experiments. Med, medium; NT, nontargeting. Scale bar: 5 μm.

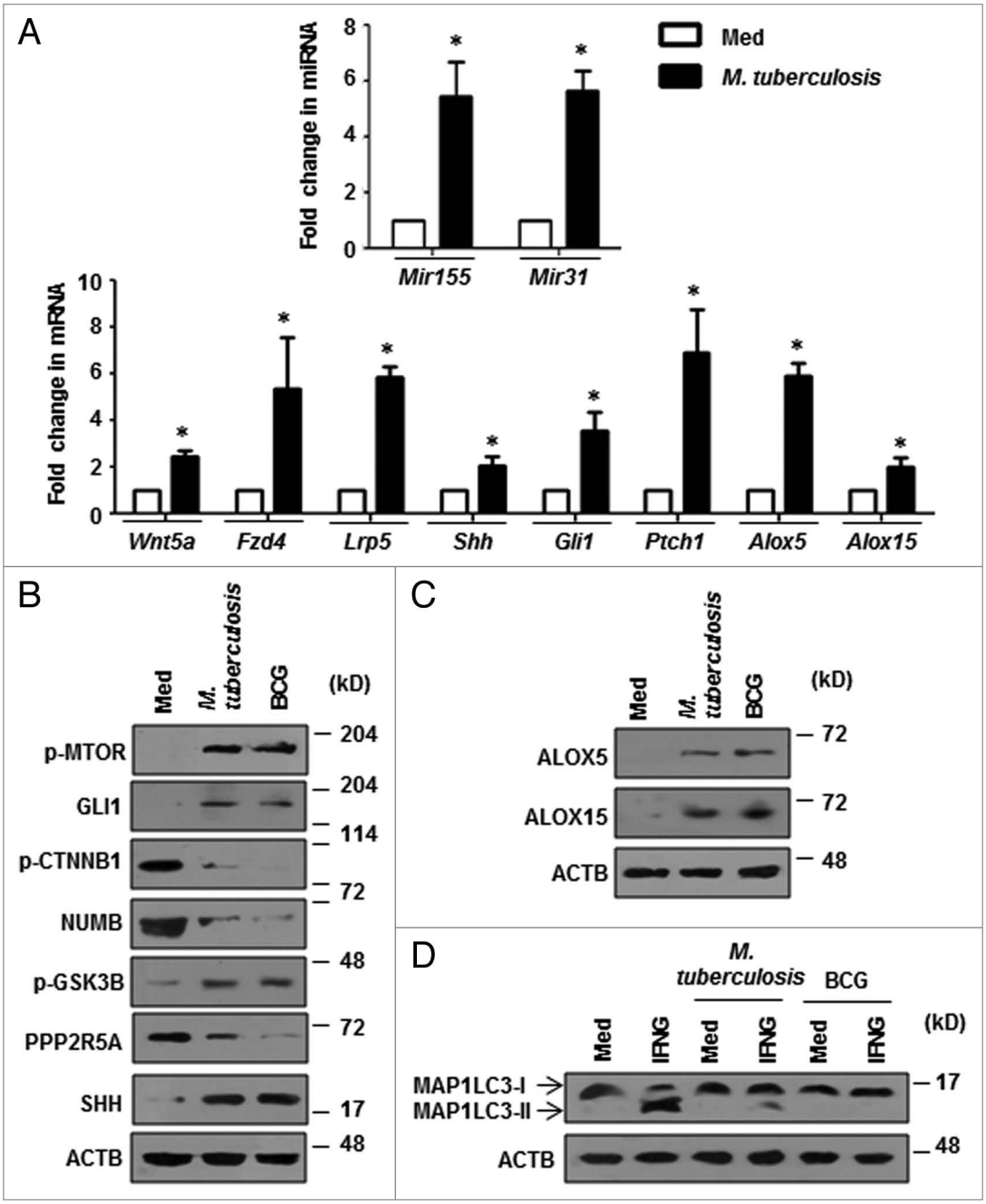

Figure 8. *M. tuberculosis* induces the *Mir155-Mir31*-WNT-SHH-ALOX pathway to inhibit autophagy. (**A**) Quantitative real-time RT-PCR for *Mir155* and *Mir31* (top panel) and WNT-SHH signaling markers and ALOXs (bottom panel) in macrophages infected with *M. tuberculosis*. (**B and C**) Immunoblotting analysis of various WNT-SHH signaling markers (**B**) and ALOXs (**C**) in macrophages infected with *M. tuberculosis* or *M. bovis* BCG. (**D**) Mouse peritoneal macrophages were infected with *M. tuberculosis* or *M. bovis* BCG for 12 h and treated with IFNG for 2 h. Immunoblots for MAP1LC3 cleavage state. All data represent the mean ± SEM for 4 values from 2 independent experiments, $^*P < 0.05$ (*t* test) and all blots are representative of 3 independent experiments. The cells were infected with bacteria at MOI 1:10 in the experiments. Med, medium.

Immunoblotting

Infected or treated macrophages were lysed in RIPA buffer constituting 50 mM TRIS-HCl (pH 7.4), 1% NP-40, 0.25% Sodium deoxycholate, 150 mM NaCl, 1 mM EDTA, 1 mM PMSF, 1 μg/ml of each aprotinin, leupeptin, pepstatin, 1 mM Na_3VO_4 and 1 mM NaF. An equal amount of protein from each cell lysate was resolved on a 12% SDS-polyacrylamide gel and transferred to polyvinylidene difluoride membranes (Millipore, IPVH00010) by the semidry transfer (Bio-Rad, 170-3940) method. Nonspecific binding was blocked with 5% nonfat dry milk powder in TBST [20 mM TRIS-HCl (pH 7.4), 137 mM NaCl, and 0.1% Tween 20] for 60 min. The blots were incubated overnight at 4 °C with primary antibody followed by incubation with anti-rabbit-HRP or

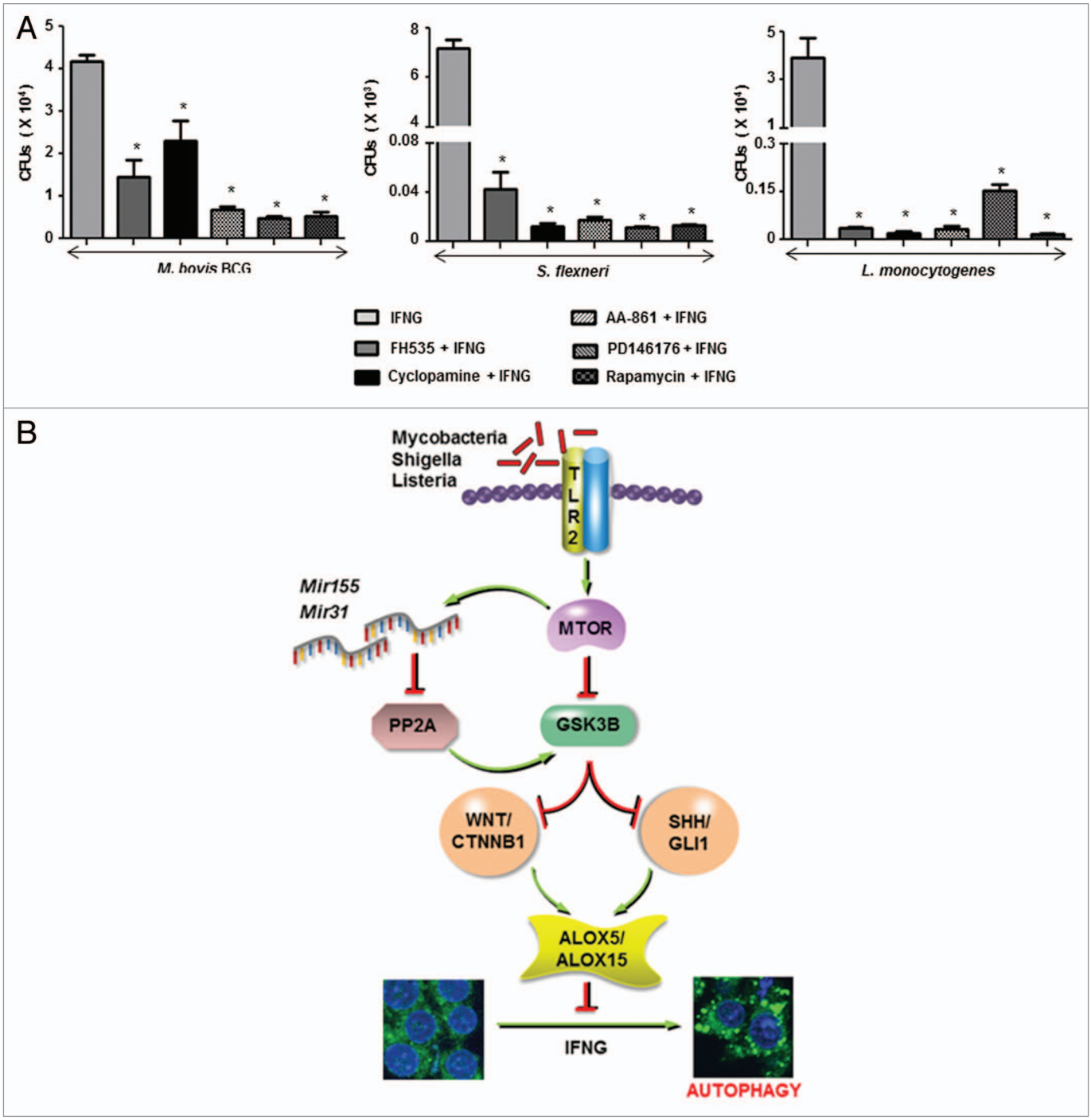

Figure 9. The WNT-SHH-ALOX pathway protects bacteria during IFNG-induced autophagy. (**A**) Peritoneal macrophages from C3H/HeJ mice pretreated with FH535 (CTNNB1/TCF inhibitor), Cyclopamine (SMO inhibitor), AA-861 (ALOX5 inhibitor), PD146176 (ALOX15 inhibitor) or Rapamycin (MTOR inhibitor) were infected with the indicated bacteria for 12 h and treated with IFNG for 18 h. To determine the bacterial survival, macrophages were lysed and quantitative real-time RT-PCR based method for CFU determination was followed. (**B**) Model: Bacteria like *Mycobacteria, Shigella*, and *Listeria* induce an MTOR-dependent upregulation in *Mir155* and *Mir31* levels which target and regulate PP2A in the macrophages. This fine-tuning of PP2A-GSK3B directs and sustains the activation of WNT-SHH-ALOX axis to inhibit IFNG-induced autophagy. All data represent the mean ± SEM for 5 to 6 values from 3 independent experiments, $^*P < 0.005$ (one-way ANOVA).

anti-mouse-HRP secondary antibody in 5% BSA for 2 h. After washing in TBST, the immunoblots were developed with enhanced chemiluminescence detection system (Perkin Elmer, NEL105001EA) as per the manufacturer's instructions. ACTB was used as loading control. For probing another protein in the same region of the PVDF membrane, the blots were stripped in the stripping buffer (62.5 mM TRIS-HCl (pH 6.8), 2% SDS and 0.7% β-mercaptoethanol) at 60 °C on a shaker, blocked

with 5% nonfat dry milk powder and probed with antibodies as mentioned above.

Luciferase assays

Cells were lysed in Reporter lysis buffer (Promega, E4030) and assayed for luciferase activity using Luciferase Assay Reagent (Promega, E4030) as per the manufacturer's instructions. The results were normalized for transfection efficiencies measured by GLB1 activity. O-nitrophenol β-D-galactopyranoside (Hi-Media, RM582) was utilized for the GLB1 assay.

Chromatin immunoprecipitation assay

Chromatin immunoprecipitation (ChIP) assays were performed using a protocol provided by Upstate Biotechnology, USA, with certain modifications. Briefly, macrophages were fixed with 1.42% formaldehyde for 15 min at room temperature followed by inactivation of formaldehyde with addition of 125 mM glycine. Nuclei were isolated from macrophages using modified RIPA buffer containing 1% Triton X-100 and chromatin was sheared. Chromatin extracts containing DNA fragments with an average size of 500 bp were immunoprecipitated using anti-CTNNB1 or anti-GLI1 or anti-H3K27me3 or anti-H3K4me3 or anti-ASH2L or rabbit preimmune sera. Purified DNA was analyzed by quantitative PCR. All results were normalized to amplification of 28S rRNA. All ChIP experiments were repeated at least three times and the primers utilized are listed in **Table S1**.

Immunoprecipitation assay

Immunoprecipitation (IP) assays were performed using a protocol provided by Millipore, USA, with certain modifications. Briefly, macrophages were gently lysed in ice-cold RIPA buffer on an orbital shaker. The cell lysates were incubated with anti-PPP2R5A, anti-p-GSK3B, anti-GSK3B or rabbit preimmune sera at 4 °C for 2 h on an orbital shaker. The immunocomplexes were captured using Protein A (Bangalore Genei, 62211018005A) agarose at 4 °C for 2 h. The beads were harvested, washed, and boiled in 5× Laemmli buffer for 10 min. The samples were separated by SDS–PAGE and further subjected for immunoblotting.

RNA immunoprecipitation

Infected BMDMs were lysed in 300 μl of complete polysomal lysis buffer (5 mM $MgCl_2$, 0.1 M KCl, 0.5% NP40, 0.01M HEPES pH 7.5). Total cell lysate (200 μg) was diluted to 500 μl using complete polysomal lysis buffer for IP. 50 μl of anti-mouse IgG precleared lysate was used as Input for the experiment and total RNA was isolated as described earlier. The rest of the precleared lysate was incubated with 1 μg anti-mouse IgG or anti-AGO2 prebound Protein A beads overnight. Further, beads were washed in complete polysomal lysis buffer and 25% of the beads were eluted in 5× Laemmli buffer for immunoblotting with anti-AGO2. The remaining beads were eluted in TRI reagent and processed for RNA isolation as described earlier. 500 ng of the RNA was converted into cDNA and quantitative real-time RT-PCR was performed to analyze *Ppp2r5A*. *Gapdh* from Input was utilized for normalization. TaqMan miRNA assays were used to quantify *Mir155*, *Mir31*, and *Mir106a* levels. U6 from Input was utilized for normalization.

Intracellular bacterial CFUs

Two million/well C3H/HeJ mouse macrophages were seeded in 12-well plates and treated with respective inhibitors for 1 h. After 2 h of the bacterial infection, the cells were thoroughly washed with PBS and treated with gentamycin (10 μg/ml) for 2 h to kill the extracellular bacteria. The cells remained infected for further 10 h and IFNG (200 U/ml) treatment was performed for next 18 h. Macrophages were thoroughly washed with PBS and lysed in 0.1% Triton X-100. For Ct based CFU analysis, intracellular bacteria were collected and boiled at 95 °C for 20 min and sonicated (40% duty, 20 pulses). The supernatant was utilized for quantitative real-time RT-PCR using bacterial specific primers as listed in **Table S1**. Known CFUs of bacteria were utilized to generate the standard curves for CFU vs Ct.

Statistical analysis

Levels of significance for comparison between samples were determined by the Student *t* test distribution and one-way ANOVA. The data in the graphs are expressed as the mean ± SE for 5 or 6 values from 3 independent experiments and *P* values < 0.05 were defined as significant. Graphpad Prism 5.0 software (Graphpad Software) was used for all the statistical analysis.

Disclosure of Potential Conflicts of Interest

No potential conflicts of interest needed to be disclosed.

Acknowledgments

We thank the Central Animal facility, Indian Institute of Science (IISc) for providing mice for experimentation and Samrajyam Nara and Pannaga of the MCB, IISc confocal facility for generous help. We acknowledge Dr Devram Sampat Ghorpade, Dr Kushagra Bansal, Shambhuprasad TK, Jamma Trinath and Dr Yeddula Narayana for critical comments and timely help during the current course of investigation. We sincerely thank Dr Douglas Golenbock, University of Massachusetts Medical School, Worcester, MA USA for the TLR2 DN construct, Dr Peter Houghton, The Research Institute at Nationwide Children's Hospital, OH USA for MTOR DN and overexpression constructs and Dr Gautam Das and Dr EH Baehrecke, University of Massachusetts Medical School, Worcester, MA USA for the pEGFP-LC3 construct. Dr Roel Nusse, Stanford University Medical Center, CA USA; Dr Andrew McMahon, Harvard University, MA USA; Dr Stefan Strack, University of Iowa College of Medicine, IA USA and Dr Colin D Funk, Queen's University, Kingston, CA are acknowledged for kind gifts of WNT5A, SHH, PPP2R5A, ALOX5, and ALOX15 overexpression constructs respectively. The *Alox5* promoter luciferase construct was provided by Dr Dieter Steinhilber, Institute of Pharmaceutical Chemistry, Frankfurt, Germany. We thank Dr Iain McInnes, University of Glasgow, Scotland UK, for sharing *mir155*-KO mice. We acknowledge Dr Usha Vijayraghavan, Dr Annapoorni Rangarajan, Dr Kumaravel Somasundaram, and Dr Saibal Chatterjee for their kind help.

This study is supported by funds from the Department of Biotechnology (DBT), Department of Science and Technology (DST), Council for Scientific and Industrial Research (CSIR) and Indian Council of Medical Research (ICMR) and

Government of India and the Indo-French Center for Promotion of Advanced Research (IFCPAR/CEFIPRA). Infrastructure support from ICMR (Center for advanced study in Molecular Medicine), DST (FIST) and UGC (special assistance) (KNB); fellowship from IISc (SH) are acknowledged.

Supplemental Materials

Supplemental materials may be found here:
www.landesbioscience.com/journals/autophagy/article/27225

References

1. Yorimitsu T, Klionsky DJ. Atg11 links cargo to the vesicle-forming machinery in the cytoplasm to vacuole targeting pathway. Mol Biol Cell 2005; 16:1593-605; PMID:15659643; http://dx.doi.org/10.1091/mbc.E04-11-1035
2. Mariño G, López-Otín C. Autophagy: molecular mechanisms, physiological functions and relevance in human pathology. Cell Mol Life Sci 2004; 61:1439-54; PMID:15197469; http://dx.doi.org/10.1007/s00018-004-4012-4
3. Yang Z, Klionsky DJ. An overview of the molecular mechanism of autophagy. Curr Top Microbiol Immunol 2009; 335:1-32; PMID:19802558; http://dx.doi.org/10.1007/978-3-642-00302-8_1
4. Levine B, Klionsky DJ. Development by self-digestion: molecular mechanisms and biological functions of autophagy. Dev Cell 2004; 6:463-77; PMID:15068787; http://dx.doi.org/10.1016/S1534-5807(04)00099-1
5. Shintani T, Klionsky DJ. Autophagy in health and disease: a double-edged sword. Science 2004; 306:990-5; PMID:15528435; http://dx.doi.org/10.1126/science.1099993
6. Deretic V. Autophagy in innate and adaptive immunity. Trends Immunol 2005; 26:523-8; PMID:16099218; http://dx.doi.org/10.1016/j.it.2005.08.003
7. Levine B, Deretic V. Unveiling the roles of autophagy in innate and adaptive immunity. Nat Rev Immunol 2007; 7:767-77; PMID:17767194; http://dx.doi.org/10.1038/nri2161
8. Castillo EF, Dekonenko A, Arko-Mensah J, Mandell MA, Dupont N, Jiang S, Delgado-Vargas M, Timmins GS, Bhattacharya D, Yang H, et al. Autophagy protects against active tuberculosis by suppressing bacterial burden and inflammation. Proc Natl Acad Sci U S A 2012; 109:E3168-76; PMID:23093667; http://dx.doi.org/10.1073/pnas.1210500109
9. Bradfute SB, Castillo EF, Arko-Mensah J, Chauhan S, Jiang S, Mandell M, Deretic V. Autophagy as an immune effector against tuberculosis. Curr Opin Microbiol 2013; 16:355-65; PMID:23790398; http://dx.doi.org/10.1016/j.mib.2013.05.003
10. Levine B, Mizushima N, Virgin HW. Autophagy in immunity and inflammation. Nature 2011; 469:323-35; PMID:21248839; http://dx.doi.org/10.1038/nature09782
11. Kirkegaard K, Taylor MP, Jackson WT. Cellular autophagy: surrender, avoidance and subversion by microorganisms. Nat Rev Microbiol 2004; 2:301-14; PMID:15031729; http://dx.doi.org/10.1038/nrmicro865
12. Orvedahl A, Levine B. Viral evasion of autophagy. Autophagy 2008; 4:280-5; PMID:18059171
13. Zullo AJ, Lee S. Mycobacterial induction of autophagy varies by species and occurs independently of mammalian target of rapamycin inhibition. J Biol Chem 2012; 287:12668-78; PMID:22275355; http://dx.doi.org/10.1074/jbc.M111.320135
14. Ogawa M, Yoshimori T, Suzuki T, Sagara H, Mizushima N, Sasakawa C. Escape of intracellular Shigella from autophagy. Science 2005; 307:727-31; PMID:15576571; http://dx.doi.org/10.1126/science.1106036
15. Yoshikawa Y, Ogawa M, Hain T, Yoshida M, Fukumatsu M, Kim M, Mimuro H, Nakagawa I, Yanagawa T, Ishii T, et al. Listeria monocytogenes ActA-mediated escape from autophagic recognition. Nat Cell Biol 2009; 11:1233-40; PMID:19749745; http://dx.doi.org/10.1038/ncb1967
16. Kumar D, Nath L, Kamal MA, Varshney A, Jain A, Singh S, Rao KV. Genome-wide analysis of the host intracellular network that regulates survival of Mycobacterium tuberculosis. Cell 2010; 140:731-43; PMID:20211141; http://dx.doi.org/10.1016/j.cell.2010.02.012
17. Delgado MA, Elmaoued RA, Davis AS, Kyei G, Deretic V. Toll-like receptors control autophagy. EMBO J 2008; 27:1110-21; PMID:18337753; http://dx.doi.org/10.1038/emboj.2008.31
18. Narayana Y, Balaji KN. NOTCH1 up-regulation and signaling involved in Mycobacterium bovis BCG-induced SOCS3 expression in macrophages. J Biol Chem 2008; 283:12501-11; PMID:18332140; http://dx.doi.org/10.1074/jbc.M709960200
19. Bansal K, Trinath J, Chakravortty D, Patil SA, Balaji KN. Pathogen-specific TLR2 protein activation programs macrophages to induce Wnt-beta-catenin signaling. J Biol Chem 2011; 286:37032-44; PMID:21862586; http://dx.doi.org/10.1074/jbc.M111.260414
20. Ghorpade DS, Holla S, Kaveri SV, Bayry J, Patil SA, Balaji KN. Sonic hedgehog-dependent induction of microRNA 31 and microRNA 150 regulates Mycobacterium bovis BCG-driven toll-like receptor 2 signaling. Mol Cell Biol 2013; 33:543-56; PMID:23166298; http://dx.doi.org/10.1128/MCB.01108-12
21. Thoma-Uszynski S, Stenger S, Takeuchi O, Ochoa MT, Engele M, Sieling PA, Barnes PF, Rollinghoff M, Bolcskei PL, Wagner M, et al. Induction of direct antimicrobial activity through mammalian toll-like receptors. Science 2001; 291:1544-7; PMID:11222859; http://dx.doi.org/10.1126/science.291.5508.1544
22. Jimenez-Sanchez M, Menzies FM, Chang YY, Simecek N, Neufeld TP, Rubinsztein DC. The Hedgehog signalling pathway regulates autophagy. Nat Commun 2012; 3:1200; PMID:23149744; http://dx.doi.org/10.1038/ncomms2212
23. Djavaheri-Mergny M, Amelotti M, Mathieu J, Besançon F, Bauvy C, Souquère S, Pierron G, Codogno P. NF-kappaB activation represses tumor necrosis factor-alpha-induced autophagy. J Biol Chem 2006; 281:30373-82; PMID:16857678; http://dx.doi.org/10.1074/jbc.M602097200
24. Gutierrez MG, Master SS, Singh SB, Taylor GA, Colombo MI, Deretic V. Autophagy is a defense mechanism inhibiting BCG and Mycobacterium tuberculosis survival in infected macrophages. Cell 2004; 119:753-66; PMID:15607973; http://dx.doi.org/10.1016/j.cell.2004.11.038
25. Pyo JO, Jang MH, Kwon YK, Lee HJ, Jun JI, Woo HN, Cho DH, Choi B, Lee H, Kim JH, et al. Essential roles of Atg5 and FADD in autophagic cell death: dissection of autophagic cell death into vacuole formation and cell death. J Biol Chem 2005; 280:20722-9; PMID:15778222; http://dx.doi.org/10.1074/jbc.M413934200
26. Harris J, De Haro SA, Master SS, Keane J, Roberts EA, Delgado M, Deretic V. T helper 2 cytokines inhibit autophagic control of intracellular Mycobacterium tuberculosis. Immunity 2007; 27:505-17; PMID:17892853; http://dx.doi.org/10.1016/j.immuni.2007.07.022
27. Pathak SK, Bhattacharyya A, Pathak S, Basak C, Mandal D, Kundu M, Basu J. Toll-like receptor 2 and mitogen- and stress-activated kinase 1 are effectors of Mycobacterium avium-induced cyclooxygenase-2 expression in macrophages. J Biol Chem 2004; 279:55127-36; PMID:15496409; http://dx.doi.org/10.1074/jbc.M409885200
28. Bansal K, Narayana Y, Patil SA, Balaji KN. M. bovis BCG induced expression of COX-2 involves nitric oxide-dependent and -independent signaling pathways. J Leukoc Biol 2009; 85:804-16; PMID:19228814; http://dx.doi.org/10.1189/jlb.0908561
29. Kam Y, Exton JH. Role of phospholipase D1 in the regulation of mTOR activity by lysophosphatidic acid. FASEB J 2004; 18:311-9; PMID:14769825; http://dx.doi.org/10.1096/fj.03-0731com
30. Garcia A, Zheng Y, Zhao C, Toschi A, Fan J, Shraibman N, Brown HA, Bar-Sagi D, Foster DA, Arbiser JL. Honokiol suppresses survival signals mediated by Ras-dependent phospholipase D activity in human cancer cells. Clin Cancer Res 2008; 14:4267-74; PMID:18594009; http://dx.doi.org/10.1158/1078-0432.CCR-08-0102
31. Dal Col J, Dolcetti R. GSK-3beta inhibition: at the crossroad between Akt and mTOR constitutive activation to enhance cyclin D1 protein stability in mantle cell lymphoma. Cell Cycle 2008; 7:2813-6; PMID:18769147; http://dx.doi.org/10.4161/cc.7.18.6733
32. Bhatia B, Northcott PA, Hambardzumyan D, Govindarajan B, Brat DJ, Arbiser JL, Holland EC, Taylor MD, Kenney AM. Tuberous sclerosis complex suppression in cerebellar development and medulloblastoma: separate regulation of mammalian target of rapamycin activity and p27 Kip1 localization. Cancer Res 2009; 69:7224-34; PMID:19738049; http://dx.doi.org/10.1158/0008-5472.CAN-09-1299
33. Hernández F, Langa E, Cuadros R, Avila J, Villanueva N. Regulation of GSK3 isoforms by phosphatases PP1 and PP2A. Mol Cell Biochem 2010; 344:211-5; PMID:20652371; http://dx.doi.org/10.1007/s11010-010-0544-0
34. Gao ZH, Seeling JM, Hill V, Yochum A, Virshup DM. Casein kinase I phosphorylates and destabilizes the beta-catenin degradation complex. Proc Natl Acad Sci U S A 2002; 99:1182-7; PMID:11818547; http://dx.doi.org/10.1073/pnas.032468199
35. Seeling JM, Miller JR, Gil R, Moon RT, White R, Virshup DM. Regulation of beta-catenin signaling by the B56 subunit of protein phosphatase 2A. Science 1999; 283:2089-91; PMID:10092233; http://dx.doi.org/10.1126/science.283.5410.2089
36. Li X, Yost HJ, Virshup DM, Seeling JM. Protein phosphatase 2A and its B56 regulatory subunit inhibit Wnt signaling in Xenopus. EMBO J 2001; 20:4122-31; PMID:11483515; http://dx.doi.org/10.1093/emboj/20.15.4122
37. Krauss S, Foerster J, Schneider R, Schweiger S. Protein phosphatase 2A and rapamycin regulate the nuclear localization and activity of the transcription factor GLI3. Cancer Res 2008; 68:4658-65; PMID:18559511; http://dx.doi.org/10.1158/0008-5472.CAN-07-6174
38. Jin Z, Mei W, Strack S, Jia J, Yang J. The antagonistic action of B56-containing protein phosphatase 2As and casein kinase 2 controls the phosphorylation and Gli turnover function of Daz interacting protein 1. J Biol Chem 2011; 286:36171-9; PMID:21878643; http://dx.doi.org/10.1074/jbc.M111.274761
39. Sauer S, Bruno L, Hertweck A, Finlay D, Leleu M, Spivakov M, Knight ZA, Cobb BS, Cantrell D, O'Connor E, et al. T cell receptor signaling controls Foxp3 expression via PI3K, Akt, and mTOR. Proc Natl Acad Sci U S A 2008; 105:7797-802; PMID:18509048; http://dx.doi.org/10.1073/pnas.0800928105

40. Netea MG, Van der Meer JW, Sutmuller RP, Adema GJ, Kullberg BJ. From the Th1/Th2 paradigm towards a Toll-like receptor/T-helper bias. Antimicrob Agents Chemother 2005; 49:3991-6; PMID:16189071; http://dx.doi.org/10.1128/AAC.49.10.3991-3996.2005
41. Bansal K, Sinha AY, Ghorpade DS, Togarsimalemath SK, Patil SA, Kaveri SV, Balaji KN, Bayry J. Src homology 3-interacting domain of Rv1917c of Mycobacterium tuberculosis induces selective maturation of human dendritic cells by regulating PI3K-MAPK-NF-kappaB signaling and drives Th2 immune responses. J Biol Chem 2010; 285:36511-22; PMID:20837474; http://dx.doi.org/10.1074/jbc.M110.158055
42. Serhan CN, Chiang N, Van Dyke TE. Resolving inflammation: dual anti-inflammatory and pro-resolution lipid mediators. Nat Rev Immunol 2008; 8:349-61; PMID:18437155; http://dx.doi.org/10.1038/nri2294
43. Aliberti J, Bafica A. Anti-inflammatory pathways as a host evasion mechanism for pathogens. Prostaglandins Leukot Essent Fatty Acids 2005; 73:283-8; PMID:15982863; http://dx.doi.org/10.1016/j.plefa.2005.05.018
44. Fabri M, Stenger S, Shin DM, Yuk JM, Liu PT, Realegeno S, Lee HM, Krutzik SR, Schenk M, Sieling PA, et al. Vitamin D is required for IFN-gamma-mediated antimicrobial activity of human macrophages. Sci Transl Med 2011; 3:ra102; PMID:21998409; http://dx.doi.org/10.1126/scitranslmed.3003045
45. Banaiee N, Kincaid EZ, Buchwald U, Jacobs WR Jr., Ernst JD. Potent inhibition of macrophage responses to IFN-gamma by live virulent Mycobacterium tuberculosis is independent of mature mycobacterial lipoproteins but dependent on TLR2. J Immunol 2006; 176:3019-27; PMID:16493060
46. Ting LM, Kim AC, Cattamanchi A, Ernst JD. Mycobacterium tuberculosis inhibits IFN-gamma transcriptional responses without inhibiting activation of STAT1. J Immunol 1999; 163:3898-906; PMID:10490990
47. Flynn JL. Why is IFN-gamma insufficient to control tuberculosis? Trends Microbiol 1999; 7:477-8, author reply 478-9; PMID:10603481; http://dx.doi.org/10.1016/S0966-842X(99)01611-X
48. Pennini ME, Pai RK, Schultz DC, Boom WH, Harding CV. Mycobacterium tuberculosis 19-kDa lipoprotein inhibits IFN-gamma-induced chromatin remodeling of MHC2TA by TLR2 and MAPK signaling. J Immunol 2006; 176:4323-30; PMID:16547269
49. Nagabhushanam V, Solache A, Ting LM, Escaron CJ, Zhang JY, Ernst JD. Innate inhibition of adaptive immunity: Mycobacterium tuberculosis-induced IL-6 inhibits macrophage responses to IFN-gamma. J Immunol 2003; 171:4750-7; PMID:14568951
50. Fortune SM, Solache A, Jaeger A, Hill PJ, Belisle JT, Bloom BR, Rubin EJ, Ernst JD. Mycobacterium tuberculosis inhibits macrophage responses to IFN-gamma through myeloid differentiation factor 88-dependent and -independent mechanisms. J Immunol 2004; 172:6272-80; PMID:15128816
51. Pai RK, Pennini ME, Tobian AA, Canaday DH, Boom WH, Harding CV. Prolonged toll-like receptor signaling by Mycobacterium tuberculosis and its 19-kilodalton lipoprotein inhibits gamma interferon-induced regulation of selected genes in macrophages. Infect Immun 2004; 72:6603-14; PMID:15501793; http://dx.doi.org/10.1128/IAI.72.11.6603-6614.2004
52. Imai K, Kurita-Ochiai T, Ochiai K. Mycobacterium bovis bacillus Calmette-Guérin infection promotes SOCS induction and inhibits IFN-gamma-stimulated JAK/STAT signaling in J774 macrophages. FEMS Immunol Med Microbiol 2003; 39:173-80; PMID:14625101; http://dx.doi.org/10.1016/S0928-8244(03)00231-1
53. Vázquez N, Greenwell-Wild T, Rekka S, Orenstein JM, Wahl SM. Mycobacterium avium-induced SOCS contributes to resistance to IFN-gamma-mediated mycobactericidal activity in human macrophages. J Leukoc Biol 2006; 80:1136-44; PMID:16943387; http://dx.doi.org/10.1189/jlb.0306206
54. Dominici S, Schiavano GF, Magnani M, Buondelmonte C, Celeste AG, Brandi G. Involvement of Stat1 in the phagocytosis of M. avium. Clin Dev Immunol 2012; 2012:652683; PMID:22811740; http://dx.doi.org/10.1155/2012/652683
55. Dupuis S, Döffinger R, Picard C, Fieschi C, Altare F, Jouanguy E, Abel L, Casanova JL. Human interferon-gamma-mediated immunity is a genetically controlled continuous trait that determines the outcome of mycobacterial invasion. Immunol Rev 2000; 178:129-37; PMID:11213797; http://dx.doi.org/10.1034/j.1600-065X.2000.17810.x
56. Dupuis S, Jouanguy E, Al-Hajjar S, Fieschi C, Al-Mohsen IZ, Al-Jumaah S, Yang K, Chapgier A, Eidenschenk C, Eid P, et al. Impaired response to interferon-alpha/beta and lethal viral disease in human STAT1 deficiency. Nat Genet 2003; 33:388-91; PMID:12590259; http://dx.doi.org/10.1038/ng1097
57. Esquivel-Solís H, Quiñones-Falconi F, Zarain-Herzberg A, Amieva-Fernández RI, López-Vidal Y. Impaired activation of Stat1 and c-Jun as a possible defect in macrophages of patients with active tuberculosis. Clin Exp Immunol 2009; 158:45-54; PMID:19737230; http://dx.doi.org/10.1111/j.1365-2249.2009.03985.x
58. Kim HJ, Chung DH, Kim MJ, Jang JH, Kim YW, Han SK, Shim YS, Yim JJ. Decreased phosphorylation of STAT-1, STAT-4 and cytokine release in MDR-TB patients with primary resistance. Int J Tuberc Lung Dis 2008; 12:1071-6; PMID:18713507
59. Young AR, Narita M, Ferreira M, Kirschner K, Sadaie M, Darot JF, Tavaré S, Arakawa S, Shimizu S, Watt FM, et al. Autophagy mediates the mitotic senescence transition. Genes Dev 2009; 23:798-803; PMID:19279323; http://dx.doi.org/10.1101/gad.519709
60. Ghorpade DS, Leyland R, Kurowska-Stolarska M, Patil SA, Balaji KN. MicroRNA-155 is required for Mycobacterium bovis BCG-mediated apoptosis of macrophages. Mol Cell Biol 2012; 32:2239-53; PMID:22473996; http://dx.doi.org/10.1128/MCB.06597-11
61. Quesniaux VJ, Nicolle DM, Torres D, Kremer L, Guérardel Y, Nigou J, Puzo G, Erard F, Ryffel B. Toll-like receptor 2 (TLR2)-dependent-positive and TLR2-independent-negative regulation of proinflammatory cytokines by mycobacterial lipomannans. J Immunol 2004; 172:4425-34; PMID:15034058
62. Bansal K, Elluru SR, Narayana Y, Chaturvedi R, Patil SA, Kaveri SV, Bayry J, Balaji KN. PE_PGRS antigens of Mycobacterium tuberculosis induce maturation and activation of human dendritic cells. J Immunol 2010; 184:3495-504; PMID:20176745; http://dx.doi.org/10.4049/jimmunol.0903299
63. Eulalio A, Schulte L, Vogel J. The mammalian microRNA response to bacterial infections. RNA Biol 2012; 9:742-50; PMID:22664920; http://dx.doi.org/10.4161/rna.20018
64. O'Connell RM, Rao DS, Baltimore D. microRNA regulation of inflammatory responses. Annu Rev Immunol 2012; 30:295-312; PMID:22224773; http://dx.doi.org/10.1146/annurev-immunol-020711-075013
65. Park IH, Yeum CE, Chae GT, Lee SB. Effect of rifampicin to inhibit rapamycin-induced autophagy via the suppression of protein phosphatase 2A activity. Immunopharmacol Immunotoxicol 2008; 30:837-49; PMID:18608530; http://dx.doi.org/10.1080/08923970802135732
66. Meske V, Albert F, Ohm TG. Coupling of mammalian target of rapamycin with phosphoinositide 3-kinase signaling pathway regulates protein phosphatase 2A- and glycogen synthase kinase-3 -dependent phosphorylation of Tau. J Biol Chem 2008; 283:100-9; PMID:17971449; http://dx.doi.org/10.1074/jbc.M704292200
67. Davis JM, Ramakrishnan L. The role of the granuloma in expansion and dissemination of early tuberculous infection. Cell 2009; 136:37-49; PMID:19135887; http://dx.doi.org/10.1016/j.cell.2008.11.014
68. Jin S, White E. Role of autophagy in cancer: management of metabolic stress. Autophagy 2007; 3:28-31; PMID:16969128
69. Yousefi S, Perozzo R, Schmid I, Ziemiecki A, Schaffner T, Scapozza L, Brunner T, Simon HU. Calpain-mediated cleavage of Atg5 switches autophagy to apoptosis. Nat Cell Biol 2006; 8:1124-32; PMID:16998475; http://dx.doi.org/10.1038/ncb1482
70. Uhlmann S, Mannsperger H, Zhang JD, Horvat EA, Schmidt C, Küblbeck M, Henjes F, Ward A, Tschulena U, Zweig K, et al. Global microRNA level regulation of EGFR-driven cell-cycle protein network in breast cancer. Mol Syst Biol 2012; 8:570; PMID:22333974; http://dx.doi.org/10.1038/msb.2011.100
71. Aliberti J, Hieny S, Reis e Sousa C, Serhan CN, Sher A. Lipoxin-mediated inhibition of IL-12 production by DCs: a mechanism for regulation of microbial immunity. Nat Immunol 2002; 3:76-82; PMID:11743584; http://dx.doi.org/10.1038/ni745
72. DiMeo D, Tian J, Zhang J, Narushima S, Berg DJ. Increased interleukin-10 production and Th2 skewing in the absence of 5-lipoxygenase. Immunology 2008; 123:250-62; PMID:17894798
73. Bafica A, Scanga CA, Serhan C, Machado F, White S, Sher A, Aliberti J. Host control of Mycobacterium tuberculosis is regulated by 5-lipoxygenase-dependent lipoxin production. J Clin Invest 2005; 115:1601-6; PMID:15931391; http://dx.doi.org/10.1172/JCI23949
74. Pai RK, Convery M, Hamilton TA, Boom WH, Harding CV. Inhibition of IFN-gamma-induced class II transactivator expression by a 19-kDa lipoprotein from Mycobacterium tuberculosis: a potential mechanism for immune evasion. J Immunol 2003; 171:175-84; PMID:12816996
75. Narayana Y, Bansal K, Sinha AY, Kapoor N, Puzo G, Gilleron M, Balaji KN. SOCS3 expression induced by PIM2 requires PKC and PI3K signaling. Mol Immunol 2009; 46:2947-54; PMID:19608279; http://dx.doi.org/10.1016/j.molimm.2009.06.019
76. Prieto P, Cuenca J, Través PG, Fernández-Velasco M, Martín-Sanz P, Boscá L. Lipoxin A4 impairment of apoptotic signaling in macrophages: implication of the PI3K/Akt and the ERK/Nrf-2 defense pathways. Cell Death Differ 2010; 17:1179-88; PMID:20094061; http://dx.doi.org/10.1038/cdd.2009.220
77. Romagnoli A, Etna MP, Giacomini E, Pardini M, Remoli ME, Corazzari M, Falasca L, Goletti D, Gafa V, Simeone R, et al. ESX-1 dependent impairment of autophagic flux by Mycobacterium tuberculosis in human dendritic cells. Autophagy 2012; 8:1357-70; PMID:22885411; http://dx.doi.org/10.4161/auto.20881
78. Thai TH, Calado DP, Casola S, Ansel KM, Xiao C, Xue Y, Murphy A, Frendewey D, Valenzuela D, Kutok JL, et al. Regulation of the germinal center response by microRNA-155. Science 2007; 316:604-8; PMID:17463289; http://dx.doi.org/10.1126/science.1141229
79. Kurowska-Stolarska M, Alivernini S, Ballantine LE, Asquith DL, Millar NL, Gilchrist DS, Reilly J, Ierna M, Fraser AR, Stolarski B, et al. MicroRNA-155 as a proinflammatory regulator in clinical and experimental arthritis. Proc Natl Acad Sci U S A 2011; 108:11193-8; PMID:21690378; http://dx.doi.org/10.1073/pnas.1019536108